Supporting Information for "Assessing Local Emission for Air Pollution via Data Experiments"

Yuru Zhu[1], Yinshuang Liang[3]and Song Xi Chen[1,2]

[1]Center for Statistical Science,

[2]Guanghua School of Management, Peking University, Beijing, 100871, China

[3]School of Information Engineering, Zhengzhou University of Technology, Henan, 450044, China

Contents of this file

Introduction This supporting information provides some additional figures that can support the analysis of this study, as well as some technical details.

Text S1.

The algorithm for calm episode selection is described in Algorithm 1.

Text S2.

We outline the conditions assumed in our study here to derive the asymptotic properties in Section 4. For a season and a site cluster, let $X_{ij} = (X_{ij1}^\top, \cdots, X_{ijT_{ij}}^\top)^\top$ be the vector of

---

Corresponding author: Song Xi Chen (csx@gsm.pku.edu.cn)

Algorithm 1: Selection of Calm Episodes

Input: Time series of wind speed $\{\mathrm{WS}_t\}_{t=1}^{L}$, cumulative northerly $\{\mathrm{CNWS}_t\}_{t=1}^{L}$ and southerly wind speed $\{\mathrm{CSWS}_t\}_{t=1}^{L}$, cumulative precipitation $\{\mathrm{R}_t\}_{t=1}^{L}$ and concentration of $\mathrm{PM}_{2.5}$ $\{\mathrm{PM2.5}_t\}_{t=1}^{L}$.

Output: Sets of starting time $\mathcal{S}$ and ending time $\mathcal{E}$ of the selected calm episodes.

Initialize: $\mathcal{S} = \mathcal{E} = \varnothing$.

Select the ending times of strong northerly processes

$\mathcal{A} = \{t_\omega | \mathrm{CNWS}_{t_\omega - 1} \geq 10.8\mathrm{m/s} \text{ and } \mathrm{CNWS}_{t_\omega} = 0\}$ and the candidate set for starting times of episodes

$\mathcal{C} = \{t | \mathrm{WS}_t \leq 5.4\mathrm{m/s}, \max\{\mathrm{PM2.5}_{t-1}, \mathrm{PM2.5}_t\} \leq 35\mu\mathrm{g/m}^3, \mathrm{R}_{t-1} = \mathrm{R}_t = 0\}$.

for $t_\omega \in \mathcal{A}$ **do**

1. $\mathcal{B}_{t_\omega} = [t_\omega - 8, t_\omega + 8] \cap (max\{t : t \in \{0\} \cup \mathcal{E}\}, L] \cap \mathcal{C}$, $t_s = \arg\min_{t \in \mathcal{B}_{t_\omega}} \mathrm{PM2.5}_t$.

2. **if** $t_s < t_\omega$ *and* $\max\{R_t | t_s < t < t_\omega\} = 0$ **then**
   $k = t_\omega$
   else if $t_s \geq t_\omega$ **then**
   $k = t_s$.
3. **while** $R_k = 0$, $CNWS_k \leq 3.3m/s$ *and* $CSWS_k \leq 13.8m/s$ **do**
   $k = k + 1$.
4. $t_e = k - 1$.

5. **if** $t_e - t_s \geq 3$ **then**
   $\mathcal{S} = \mathcal{S} \cup \{t_s\}$ and $\mathcal{E} = \mathcal{E} \cup \{t_e\}$.

selected covariates for Model (4.1) observed within T_{ij} hours for episode j. The following assumptions are needed for the statistical inference.

Assumption 1. *For different i or j, $\{(\Delta M_{ij1}^\top, \epsilon_{ij1}, \cdots, \Delta M_{ijT_{ij}}^\top, \epsilon_{ijT_{ij}}, C_{ij}^\top)^\top\}$ are mutually independent.*

Assumption 2. *For $t = 1, \cdots, T_{ij}$, $\mathbb{E}(\epsilon_{ijt}|X_{ij}) = 0$ and $\mathrm{Var}(\epsilon_{ijt}|X_{ij})$ is finite.*

Assumption 3. *(i) For each i, T_{ij} is finite and $n_i^{-1}\sum_{j=1}^{n_i}\mathrm{Var}(\sum_{t=1}^{T_{ij}} X_{ijt}\epsilon_{ijt}) \to \Omega_i$ as $n_i \to \infty$; and for all $\xi > 0$, $n_i^{-1}\sum_{j=1}^{n_i}\mathbb{E}\|\sum_{t=1}^{T_{ij}} X_{ijt}\epsilon_{ijt}\|^2 1\left\{\left\|\sum_{t=1}^{T_{ij}} X_{ijt}\epsilon_{ijt}\right\| > \xi n_i^{1/2}\right\} \to 0$. (ii) $\mathbb{E}(|X_{ijt}X_{ijt}^\top|)$ is finite for any i, j, and t. For each i, $n_i^{-1}\sum_{j=1}^{n_i}\sum_{t=1}^{T_{ij}}\mathbb{E}(X_{ijt}X_{ijt}^\top) \to \mathbf{H}_i$ for a positive definite $\mathbf{H}_i$ and $n_i^{-2}\sum_{j=1}^{n_i}\mathrm{Var}(\sum_{t=1}^{T_{ij}} X_{ijt}X_{ijt}^\top) \to 0$ as $n_i \to \infty$.*

Assumption 4. *(i) For all the calm episodes whose length is equal to l, the distributions of $(U_{ij1}^\top, \cdots, U_{ijl}^\top)^\top$ are identical. (ii) For a season and a site cluster in year i, $\frac{n_{il}}{n_i} \to p_{il}$ as $n_i \to \infty$, and $\frac{n_{il}}{\sum_{l\geq t} n_{il}} - \frac{p_{il}}{\sum_{l\geq t} p_{il}} = o(n_i^{-1/2})$ for any $1 \leq t \leq l \leq \tilde{T}_i$, where $\{p_{il}\}_{l=3}^{\tilde{T}_i}$ are a set of positive probability weights summing to one.*

Assumption 5. *As $n_i \to \infty$, $i = 1, \cdots, A$, $\frac{n_i}{\sum_{a=1}^A n_a} \to \kappa_i > 0$ where $\sum_{a=1}^A \kappa_a = 1$.*

Assumption 1 assumes the data in different episodes are independent. The strict exogeneity of X_{ij} in Assumption 2 implies ϵ_{ijt} is uncorrelated with the explanatory variables of episode j observed at all hours. Assumption 3 (i) gives the Lindeberg condition for establishing the asymptotic normal distribution of the OLS estimator, and Assumption 3 (ii) guarantees the consistency of $n_i^{-1}\sum_{j=1}^{n_i}\sum_{t=1}^{T_{ij}} X_{ijt}X_{ijt}^\top$. Assumption 4 (i) assumes the episodes with the same length share the same meteorological distribution. Assumption 4 (ii) and Assumption 5 avoid the extremely small number of episodes with length l relative to n_i in year i and the extremely small sample size in some years of a certain season in a site cluster, respectively.

Text S3.

The following theorem establishes the asymptotic normality of the OLS estimator $\hat{\theta}_i$.

Theorem 1. *Under Assumptions 1-3, $\hat{\theta}_i$ is unbiased and consistent for θ with the asymptotic normality*

$$\sqrt{n_i}(\hat{\theta}_i - \theta_i) \xrightarrow{d} \mathcal{N}\left(\mathbf{0}, \mathrm{AVar}(\hat{\theta}_i)\right),$$

where $\mathrm{AVar}(\hat{\theta}_i) = \mathbf{H}_i^{-1}\Omega_i\mathbf{H}_i^{-1}$.

Proof. Note that $\hat{\theta}_i - \theta_i = (n_i^{-1}\sum_{j=1}^{n_i}\sum_{t=1}^{T_{ij}} X_{ijt}X_{ijt}^\top)^{-1} n_i^{-1}\sum_{j=1}^{n_i}\sum_{t=1}^{T_{ij}} X_{ijt}\epsilon_{ijt}$. By Assumptions 1 and 2, $\mathbb{E}(\hat{\theta}_i - \theta_i) = 0$, thus $\hat{\theta}_i$ is unbiased.

Base on Assumption 3, $n_i^{-1}\sum_{j=1}^{n_i}\sum_{t=1}^{T_{ij}} X_{ijt}X_{ijt}^\top$ is consistent for $\mathbf{H}_i$. Furthermore, $n_i^{-1/2}\sum_{j=1}^{n_i}\sum_{t=1}^{T_{ij}} X_{ijt}\epsilon_{ijt} \xrightarrow{d} \mathcal{N}(\mathbf{0}, \Omega_i)$ follows from the Lindeberg-Feller theorem.

$$\begin{aligned}\sqrt{n_i}(\hat{\theta}_i - \theta_i) &= (n_i^{-1}\sum_{j=1}^{n_i}\sum_{t=1}^{T_{ij}} X_{ijt}X_{ijt}^\top)^{-1} n_i^{-1/2}\sum_{j=1}^{n_i}\sum_{t=1}^{T_{ij}} X_{ijt}\epsilon_{ijt} \\ &= \mathbf{H}_i^{-1} n_i^{-1/2}\sum_{j=1}^{n_i}\sum_{t=1}^{T_{ij}} X_{ijt}\epsilon_{ijt} + o_p(1)\end{aligned}$$

Therefore, $\hat{\theta}_i - \theta_i \xrightarrow{P} 0$ and the estimator $\hat{\theta}_i - \theta_i$ is asymptotic normal with mean zero and the asymptotic variance $\mathbf{H}_i^{-1}\Omega_i\mathbf{H}_i^{-1}$. □

Note that $\hat{\Omega}_i = n_i^{-1}\sum_{j=1}^{n_i}(\sum_{t=1}^{T_{ij}} X_{ijt}\hat{\epsilon}_{ijt})(\sum_{t=1}^{T_{ij}} X_{ijt}\hat{\epsilon}_{ijt})^\top$ is an estimate for Ω_i by convergence conditions for Ω_i in Assumption 3, thus we can construct a robust variance estimator

$$\widehat{\mathrm{Var}}(\hat{\theta}_i) = (\sum_{j=1}^{n_i}\sum_{t=1}^{T_{ij}} X_{ijt}X_{ijt}^\top)^{-1}[\sum_{j=1}^{n_i}(\sum_{t=1}^{T_{ij}} X_{ijt}\hat{\epsilon}_{ijt})(\sum_{t=1}^{T_{ij}} X_{ijt}\hat{\epsilon}_{ijt})^\top](\sum_{j=1}^{n_i}\sum_{t=1}^{T_{ij}} X_{ijt}X_{ijt}^\top)^{-1}.$$

Text S4.

In this section, we provide the asymptotic properties and variance estimation of $\hat{\mu}_{it}^*$. By the law of total expectation, $\mathbb{E}(U_{ajt}) = (\sum_{l\geq t} p_{al})^{-1}\sum_{l\geq t} p_{al}\mathbb{E}(U_{ajt}|T_{aj} = l)$. Let $\mathbb{E}(X_{a\cdot t}) =$

$(\mathbb{E}(U_{ajt})^\top, I_t^\top)^\top$ be the expectation of covariates at hour t for all calm episodes in year a, $\tilde{\mathbb{E}}(X_t) = \frac{1}{A}\sum_{a=1}^{A}\mathbb{E}(X_{a\cdot t})$ be the expectation under the baseline meteorological distribution with density $f_{\cdot t}$, $\bar{X}_{a\cdot t} = \frac{1}{\sum_{l\geq t} n_{al}}\sum_{s:Tas\geq t} X_{ast}$ be the average meteorological conditions at hour t during episodes in year a and $X_t^* = \frac{1}{A}\sum_{a=1}^{A}\bar{X}_{a\cdot t}$. Then, $\frac{1}{n_{al}}\sum_{s:T_{as}=l}\Delta M_{ast}$, $\frac{1}{n_{al}}\sum_{s:T_{as}=l} C_{as}$, $\bar{X}_{a\cdot t}$ and X_t^* are consistent estimators of $\mathbb{E}(\Delta M_{ajt}|T_{aj}=l)$, $\mathbb{E}(C_{aj}|T_{aj}=l)$, $\mathbb{E}(X_{a\cdot t})$ and $\tilde{\mathbb{E}}(X_t)$, respectively, according to the law of large numbers. Since

$$\hat{\mu}_{it}^* - \mu_{it}^* = X_t^{*\top}\hat{\theta}_i - \tilde{\mathbb{E}}(X_t)^\top\theta_i = [X_t^* - \tilde{\mathbb{E}}(X_t)]^\top\theta_i + X_t^{*\top}(\hat{\theta}_i - \theta_i),$$

$\hat{\mu}_{it}^*$ is also a consistent estimator of μ_{it}^*. The following theorem gives the asymptotic normality of $\hat{\mu}_{it}^*$.

Theorem 2. *Under Assumptions 1 – 5, for any $i = 1, \cdots, A$ and $t = 1, \cdots, \min_{1\leq a\leq A}\tilde{T}_a$, as $\min_{1\leq a\leq A} n_a \to \infty$,*

$$\sqrt{n_i}(\hat{\mu}_{it}^* - \mu_{it}^*) \xrightarrow{d} \mathcal{N}\left(0, \sigma_{i,t}^2\right),$$

where $\sigma_{i,t}^2 = \tilde{\mathbb{E}}(X_t)^\top\mathbf{H}_i^{-1}\Omega_i\mathbf{H}_i^{-1}\tilde{\mathbb{E}}(X_t) + \frac{1}{A^2}\sum_{a=1}^{A}\sum_{l\geq t}\frac{\kappa_i p_{al}}{\kappa_a(\sum_{l\geq t} p_{al})^2}\mathrm{Var}(X_{ast}^\top\theta_i|T_{as}=l)$.

By the plug-in principle that replaces the expectations and the variance by the corresponding estimates, a consistent estimator of $\sigma_{i,t}^2$ is

$$\hat{\sigma}_{i,t}^2 = X_t^{*\top}\widehat{\mathrm{AVar}}(\hat{\theta}_i)X_t^* + \frac{1}{A^2}\sum_{a=1}^{A}\sum_{l\geq t}\frac{n_i}{(\sum_{l\geq t} n_{al})^2}\sum_{s:T_{as}=l}[(X_{ast} - n_{al}^{-1}\sum_{s:T_{as}=l} X_{ast})^\top\hat{\theta}_i]^2,$$

where $\widehat{\mathrm{AVar}}(\hat{\theta}_i) = n_i\widehat{\mathrm{Var}}(\hat{\theta}_i)$. Thus, an estimator for the variance of $\hat{\mu}_{it}^*$ is

$$X_t^{*\top}\widehat{\mathrm{Var}}(\hat{\theta}_i)X_t^* + \frac{1}{A^2}\sum_{a=1}^{A}(\sum_{l\geq t} n_{al})^{-2}\sum_{l\geq t}\sum_{s:T_{as}=l}[(X_{ast} - n_{al}^{-1}\sum_{s:T_{as}=l} X_{ast})^\top\hat{\theta}_i]^2.$$

Proof. By Assumption 4 and Assumption 5, we have

$$\sqrt{n_i}(\mathbb{E}(\bar{X}_{a\cdot t}) - \mathbb{E}(X_{a\cdot t})) = \sum_{l\geq t}\sqrt{n_i}[\frac{n_{al}}{\sum_{l\geq t} n_{al}} - \frac{p_{al}}{\sum_{l\geq t} p_{al}}]\mathbb{E}(X_{ast}|T_{as}=l) = o_p(1). \quad (1)$$

From the CLT, we have

$$\begin{aligned}
\sqrt{n_i}(\bar{X}_{a\cdot t} - \mathbb{E}(\bar{X}_{a\cdot t})) &= \sum_{l\geq t} \frac{n_{al}}{\sum_{l\geq t} n_{al}} \sqrt{\frac{n_i n_a}{n_a n_{al}}} n_{al}^{-1/2} [\sum_{s:T_{as}=l} X_{ast} - \mathbb{E}(X_{ast}|T_{as}=l)] \\
&= \sum_{l\geq t} \frac{p_{al}}{\sum_{l\geq t} p_{al}} \sqrt{\frac{\kappa_i}{\kappa_a p_{al}}} n_{al}^{-1/2} [\sum_{s:T_{as}=l} X_{ast} - \mathbb{E}(X_{ast}|T_{as}=l)] + o_p(1) \\
&\xrightarrow{d} \mathcal{N}\left(\mathbf{0}, \sum_{l\geq t} \frac{\kappa_i p_{al}}{\kappa_a (\sum_{l\geq t} p_{al})^2} \mathrm{Var}(X_{ast}|T_{as}=l)\right). \qquad (2)
\end{aligned}$$

Thus, by adding equation (1) and equation (2) we obtain

$$\begin{aligned}
\sqrt{n_i}(\bar{X}_{a\cdot t} - \mathbb{E}(X_{a\cdot t})) &= \sqrt{n_i}(\bar{X}_{a\cdot t} - \mathbb{E}(\bar{X}_{a\cdot t})) + o_p(1) \qquad (3) \\
&\xrightarrow{d} \mathcal{N}\left(\mathbf{0}, \sum_{l\geq t} \frac{\kappa_i p_{al}}{\kappa_a (\sum_{l\geq t} p_{al})^2} \mathrm{Var}(X_{ast}|T_{as}=l)\right).
\end{aligned}$$

Using the consistency of X_t^* for $\tilde{E}(X_t)$ and equation (3), we decompose $\sqrt{n_i}(\hat{\mu}_{it}^* - \mu_{it}^*)$ by

$$\begin{aligned}
\sqrt{n_i}(\hat{\mu}_{it}^* - \mu_{it}^*) =& \tilde{\mathbb{E}}(X_t)^\top \sqrt{n_i}(\hat{\theta}_i - \theta_i) + \sqrt{n_i}[X_t^* - \tilde{\mathbb{E}}(X_t)]^\top \theta_i + [X_t^* - \tilde{\mathbb{E}}(X_t)]^\top \sqrt{n_i}(\hat{\theta}_i - \theta_i) \\
=& \tilde{\mathbb{E}}(X_t)^\top \sqrt{n_i}(\hat{\theta}_i - \theta_i) + \sqrt{n_i}[X_t^* - \tilde{\mathbb{E}}(X_t)]^\top \theta_i + o_p(1) \\
=& \tilde{\mathbb{E}}(X_t)^\top \sqrt{n_i}(\hat{\theta}_i - \theta_i) + \frac{1}{A}\sum_{a=1}^{A} \sqrt{n_i}[\bar{X}_{a\cdot t} - \mathbb{E}(X_{a\cdot t})]^\top \theta_i + o_p(1) \\
=& \tilde{\mathbb{E}}(X_t)^\top \sqrt{n_i}(\hat{\theta}_i - \theta_i) + \frac{1}{A}\sum_{a=1}^{A} \sqrt{n_i}[\bar{X}_{a\cdot t} - \mathbb{E}(\bar{X}_{a\cdot t})]^\top \theta_i + o_p(1) \\
=& \Phi_{it}^{(1)} + \Phi_{it}^{(2)} + \Phi_{it}^{(3)} + o_p(1),
\end{aligned}$$

where

$$\begin{aligned}
\Phi_{it}^{(1)} &= \tilde{\mathbb{E}}(X_t)^\top \sqrt{n_i}(\hat{\theta}_i - \theta_i), \\
\Phi_{it}^{(2)} &= \sqrt{n_i}\frac{1}{A}[\bar{X}_{i\cdot t} - \mathbb{E}(\bar{X}_{i\cdot t})]^\top \theta_i, \text{ and} \\
\Phi_{it}^{(3)} &= \sqrt{n_i}\frac{1}{A}\sum_{a\neq i}[\bar{X}_{a\cdot t} - \mathbb{E}(\bar{X}_{a\cdot t})]^\top \theta_i.
\end{aligned}$$

As for the first term, we have

$$\begin{aligned}\Phi_{it}^{(1)} =&\tilde{\mathbb{E}}(X_t)^\top (n_i^{-1}\sum_{j=1}^{n_i}\sum_{t=1}^{T_{ij}} X_{ijt}X_{ijt}^\top)^{-1} n_i^{-1/2}\sum_{j=1}^{n_i}\sum_{t=1}^{T_{ij}} X_{ijt}\epsilon_{ijt}\\ =&\tilde{\mathbb{E}}(X_t)^\top \mathbf{H}_i^{-1} n_i^{-1/2}\sum_{j=1}^{n_i}\sum_{t=1}^{T_{ij}} X_{ijt}\epsilon_{ijt} + o_p(1).\end{aligned}$$

From equation (2) we have

$$\begin{aligned}\Phi_{it}^{(1)} + \Phi_{it}^{(2)} =&\tilde{\mathbb{E}}(X_t)^\top \mathbf{H}_i^{-1} n_i^{-1/2}\sum_{j=1}^{n_i}\sum_{t=1}^{T_{ij}} X_{ijt}\epsilon_{ijt}\\ &+ \frac{1}{A}\sum_{l\geq t}\frac{\sqrt{p_{il}}}{\sum_{l\geq t} p_{il}} n_{il}^{-1/2}\sum_{s:T_{is}=l}[X_{ist}-\mathbb{E}(X_{ist}|T_{is}=l)]^\top\theta_i + o_p(1)\\ =&\sum_{l\geq t}\sum_{s:T_{is}=l}\frac{1}{A}\frac{\sqrt{p_{il}}}{\sum_{l\geq t} p_{il}} n_{il}^{-1/2}[X_{ist}-\mathbb{E}(X_{ist}|T_{is}=l)]^\top\theta_i + \tilde{\mathbb{E}}(X_t)^\top\mathbf{H}_i^{-1}n_i^{-1/2}\sum_{t=1}^{T_{is}} X_{ist}\epsilon_{ist}\\ &+\sum_{j:T_{ij}<l}\tilde{\mathbb{E}}(X_t)^\top\mathbf{H}_i^{-1}n_i^{-1/2}\sum_{t=1}^{T_{ij}} X_{ijt}\epsilon_{ijt} + o_p(1)\end{aligned}$$

Note that for s such that $T_{is}=l$,

$$\mathrm{Cov}(X_{ist'}\epsilon_{ist'}, X_{ist} - E(X_{ist}|T_{is}=l)) = 0 \text{ for any } t \text{ and } t'.$$

Let $\varsigma_i = \tilde{\mathbb{E}}(X_t)^\top\mathbf{H}_i^{-1}\Omega_i\mathbf{H}_i^{-1}\tilde{\mathbb{E}}(X_t) + \frac{1}{A^2}\sum_{l\geq t}\frac{p_{il}}{(\sum_{l\geq t}p_{il})^2}\mathrm{Var}(X_{ist}^\top\theta_i|T_{is}=l)$. Then,

$$\begin{aligned}&\sum_{l\geq t}\sum_{s:T_{is}=l}\mathrm{Var}\{\frac{1}{A}\frac{\sqrt{p_{il}}}{\sum_{l\geq t}p_{il}} n_{il}^{-1/2}[X_{ist}-\mathbb{E}(X_{ist}|T_{is}=l)]^\top\theta_i + \tilde{\mathbb{E}}(X_t)^\top\mathbf{H}_i^{-1}n_i^{-1/2}\sum_{t=1}^{T_{is}} X_{ist}\epsilon_{ist}\}\\ &+\sum_{j:T_{ij}<l}\mathrm{Var}[\tilde{\mathbb{E}}(X_t)^\top\mathbf{H}_i^{-1}n_i^{-1/2}\sum_{t=1}^{T_{ij}} X_{ijt}\epsilon_{ijt}] \to \varsigma_i \text{ as } n_i\to\infty.\end{aligned}$$

By the Lindeberg-Feller Theorem and the Slutsky's Theorem, as $n_i\to\infty$,

$$\Phi_{it}^{(1)} + \Phi_{it}^{(2)} \xrightarrow{d} \mathcal{N}(0,\varsigma_i).$$

The independence of episode data in different years results in

$$\Phi_{it}^{(3)} \xrightarrow{d} \mathcal{N}\left(0, \frac{1}{A^2}\sum_{a\neq i}\sum_{l\geq t}\frac{\kappa_i p_{al}}{\kappa_a(\sum_{l\geq t}p_{al})^2}\mathrm{Var}(X_{ast}^\top\theta_i|T_{as}=l)\right).$$

$\Phi_{it}^{(3)}$ is independent of $\Phi_{it}^{(1)} + \Phi_{it}^{(2)}$, therefore,

$$\sqrt{n_i}(\hat{\mu}_{it}^* - \mu_{it}^*) \xrightarrow{d} \mathcal{N}\left(0, \sigma_{i,t}^2\right),$$

where $\sigma_{i,t}^2 = \tilde{\mathbb{E}}(X_t)^\top \mathbf{H}_i^{-1} \Omega_i \mathbf{H}_i^{-1} \tilde{\mathbb{E}}(X_t) + \frac{1}{A^2} \sum_{a=1}^{A} \sum_{l \geq t} \frac{\kappa_i p_{al}}{\kappa_a (\sum_{l \geq t} p_{al})^2} \operatorname{Var}(X_{ast}^\top \theta_i | T_{as} = l)$.

Note that

$$n_{al}^{-1} \sum_{s:T_{as}=l} [(X_{ast} - n_{al}^{-1} \sum_{s:T_{as}=l} X_{ast})(X_{ast} - n_{al}^{-1} \sum_{s:T_{as}=l} X_{ast})^\top] \xrightarrow{P} \operatorname{Var}(X_{ast} | T_{as} = l),$$
$$X_t^* \xrightarrow{P} \tilde{\mathbb{E}}(X_t),\ \hat{\theta}_i \xrightarrow{P} \theta_i,\ \widehat{\operatorname{AVar}}(\hat{\theta}_i) \xrightarrow{P} \mathbf{H}_i^{-1} \Omega_i \mathbf{H}_i^{-1},\ \text{and}\ \frac{n_i n_{al}}{(\sum_{l \geq t} n_{al})^2} \to \frac{\kappa_i p_{al}}{\kappa_a (\sum_{l \geq t} p_{al})^2}.$$

Hence, we obtain the consistency of $\hat{\sigma}_{i,t}^2$ for $\sigma_{i,t}^2$. □

Text S5.

In order to test whether there are significant changes in the growth of air pollutants at a hour t between two years i and i', the following theorem provides the asymptotic distribution of $\hat{\mu}_{it}^* - \hat{\mu}_{i't}^*$ for two different years i and i'.

Theorem 3. *Under Assumptions 1 – 5, for $i \neq i'$, as $\min_{1 \leq a \leq A} n_a \to \infty$,*

$$\sqrt{n_i}[\hat{\mu}_{it}^* - \hat{\mu}_{i't}^* - (\mu_{it}^* - \mu_{i't}^*)] \xrightarrow{d} \mathcal{N}\left(0, \sigma_{i,i',t}^2\right) \quad \textit{where}$$

$$\begin{aligned}\sigma_{i,i',t}^2 =& \tilde{\mathbb{E}}(X_t)^\top \operatorname{AVar}(\hat{\theta}_i) \tilde{\mathbb{E}}(X_t) + \frac{\kappa_i}{\kappa_{i'}} \tilde{\mathbb{E}}(X_t)^\top \operatorname{AVar}(\hat{\theta}_{i'}) \tilde{\mathbb{E}}(X_t) \\ &+ \frac{1}{A^2} \sum_{a=1}^{A} \sum_{l \geq t} \frac{\kappa_i p_{al}}{\kappa_a (\sum_{l \geq t} p_{al})^2} \operatorname{Var}(X_{ast}^\top (\theta_i - \theta_{i'}) | T_{as} = l).\end{aligned}$$

A consistent estimator of $\sigma_{i,i',t}^2$ is

$$\begin{aligned}\hat{\sigma}_{i,i',t}^2 =& X_t^{*\top} [\widehat{\operatorname{AVar}}(\hat{\theta}_i) + \frac{n_i}{n_{i'}} \widehat{\operatorname{AVar}}(\hat{\theta}_{i'})] X_t^* \\ &+ \frac{1}{A^2} \sum_{a=1}^{A} \sum_{l \geq t} \frac{n_i}{(\sum_{l \geq t} n_{al})^2} \sum_{s:T_{as}=l} [(X_{ast} - n_{al}^{-1} \sum_{s:T_{as}=l} X_{ast})^\top (\hat{\theta}_i - \hat{\theta}_{i'})]^2.\end{aligned}$$

Therefore, an estimator for the variance of $\hat{\mu}^*_{it} - \hat{\mu}^*_{i't}$ is

$$\begin{aligned}\hat{\sigma}^2_{i,i',t} =& X_t^{*\top}[\widehat{\mathrm{Var}}(\hat{\theta}_i) + \widehat{\mathrm{Var}}(\hat{\theta}_{i'})]X_t^* \\ &+ \frac{1}{A^2}\sum_{a=1}^{A}(\sum_{l\geq t} n_{al})^{-2}\sum_{l\geq t}\sum_{s:T_{as}=l}[(X_{ast} - n_{al}^{-1}\sum_{s:T_{as}=l} X_{ast})^\top(\hat{\theta}_i - \hat{\theta}_{i'})]^2.\end{aligned}$$

Proof. Similarly, $\sqrt{n_i}[\hat{\mu}^*_{it} - \mu^*_{it} - (\hat{\mu}^*_{i't} - \mu^*_{i't})] = \Psi^{(1)}_{it} + \Psi^{(2)}_{it} + \Psi^{(3)}_{it} + o_p(1)$, where

$$\begin{aligned}\Psi^{(1)}_{it} =& \tilde{\mathbb{E}}(X_t)^\top\sqrt{n_i}(\hat{\theta}_i - \theta_i) + \sqrt{n_i}\frac{1}{A}[\bar{X}_{i\cdot t} - \mathbb{E}(\bar{X}_{i\cdot t})]^\top(\theta_i - \theta_{i'}) \\ \Psi^{(2)}_{it} =& -\sqrt{\frac{\kappa_i}{\kappa_{i'}}}\tilde{\mathbb{E}}(X_t)^\top\sqrt{n_{i'}}(\hat{\theta}_{i'} - \theta_{i'}) + \sqrt{n_i}\frac{1}{A}[\bar{X}_{i'\cdot t} - \mathbb{E}(\bar{X}_{i'\cdot t})]^\top(\theta_i - \theta_{i'}) \\ \Psi^{(3)}_{i} =& \sqrt{n_i}\frac{1}{A}\sum_{a\neq i,i'}[\bar{X}_{a\cdot t} - \mathbb{E}(\bar{X}_{a\cdot t})]^\top(\theta_i - \theta_{i'}).\end{aligned}$$

These three terms are independent and their asymptotic distributions are normal, with the proof mirroring the one used for Theorem 2.

$$\Psi^{(1)}_{it} \xrightarrow{d} \mathcal{N}\left(0, \tilde{\mathbb{E}}(X_t)^\top \mathrm{AVar}(\hat{\theta}_i)\tilde{\mathbb{E}}(X_t) + \frac{1}{A^2}\sum_{l\geq t}\frac{p_{il}}{(\sum_{l\geq t} p_{il})^2}\mathrm{Var}(X_{ist}^\top(\theta_i - \theta_{i'})|T_{is} = l)\right)$$

$$\Psi^{(2)}_{it} \xrightarrow{d} \mathcal{N}\left(0, \frac{\kappa_i}{\kappa_{i'}}\tilde{\mathbb{E}}(X_t^\top)\,\mathrm{AVar}(\hat{\theta}_{i'})\tilde{\mathbb{E}}(X_t) + \frac{1}{A^2}\sum_{l\geq t}\frac{\kappa_i p_{i'l}}{\kappa_{i'}(\sum_{l\geq t} p_{i'l})^2}\mathrm{Var}(X_{i'st}^\top(\theta_i - \theta_{i'})|T_{i's} = l)\right)$$

$$\Psi^{(3)}_{it} \xrightarrow{d} \mathcal{N}\left(0, \frac{1}{A^2}\sum_{a\neq i,i'}\sum_{l\geq t}\frac{\kappa_i p_{al}}{\kappa_a(\sum_{l\geq t} p_{al})^2}\mathrm{Var}(X_{ast}^\top(\theta_i - \theta_{i'})|T_{as} = l)\right).$$

Hence, $\hat{\mu}^*_i - \hat{\mu}^*_{i'}$ is asymptotic normal $\mathcal{N}\left(\mathbf{0}, \sigma^2_{i,i',t}\right)$. And by the same argument as used to prove the consistency of $\hat{\sigma}^2_{i,t}$ in the proof of Theorem 2, we can verify the consistency of $\hat{\sigma}^2_{i,i',t}$ for $\sigma^2_{i,i',t}$.

□

To compare the grow rate of pollutants μ^*_{iT}/T in the first T hours of the episodes in different years, it is essential to compare μ^*_{iT} over different years. For testing the yearly difference hypotheses $H_0 : \mu^*_{iT} = \mu^*_{i'T}$ versus $H_1 : \mu^*_{iT} > \mu^*_{i'T}$(or $\mu^*_{iT} < \mu^*_{i'T}$) at a significance level α, we use the test statistic $V_{i,i',T} = \sqrt{n_i}[\hat{\mu}^*_{iT} - \hat{\mu}^*_{i'T}]/\hat{\sigma}_{i,i',T}$, and reject the

null hypothesis, if the p-value $1 - \Phi(|V_{i,i',T}|) < \alpha$, where Φ is the cumulative distribution function of the standard normal distribution.

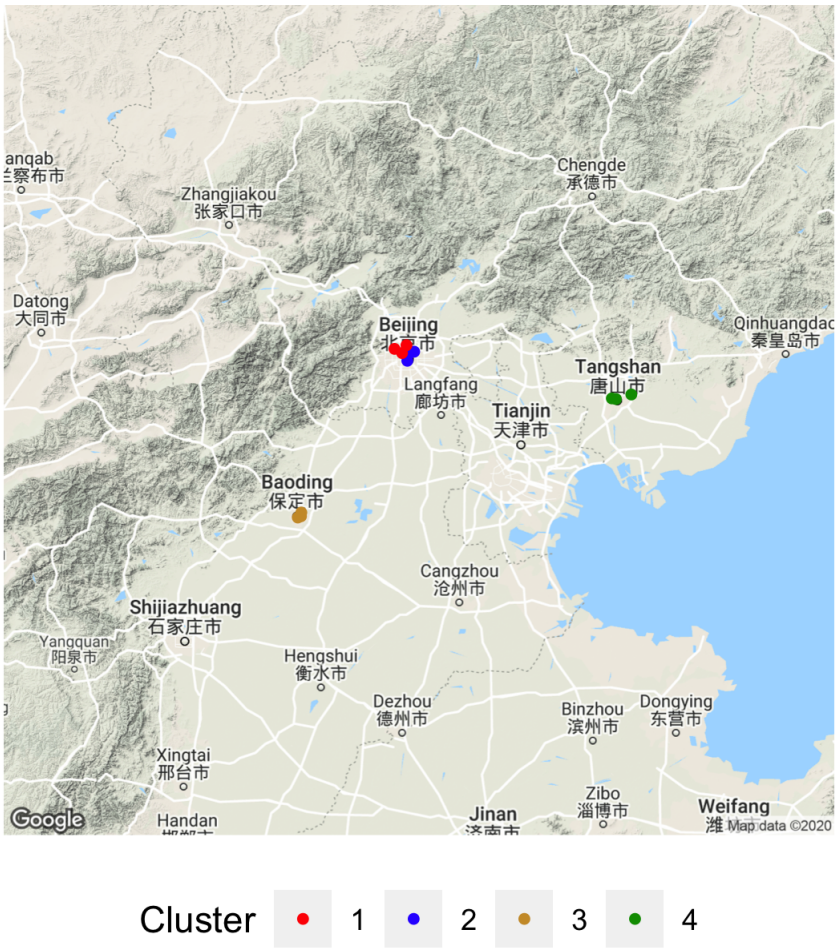

Figure S1: The northern portion of the NCP that encompasses Beijing, Baoding and Tangshan and the locations of air-quality monitoring sites in the four clusters.

	Cluster	Location	Air-quality monitoring sites	CMA station
1	Beijng SE	Southeast of the central Beijing	Dongsi, Nongzhanguan and Tiantan	Chaoyang
2	Beijng NW	Northwest of the central Beijing	Aotizhongxin, Guanyuan and Wanliu	Haidian
3	Tangshan	Tangshan	Leidazhan, Shierzhong and Wuziju	Tangshan
4	Baoding	Baoding	Huadianerqu, Jiancezhan and Youyongguan	Baoding

Table S1: Information for the four site-clusters in Beijing, Baoding and Tangshan.

(a) Beijing SE

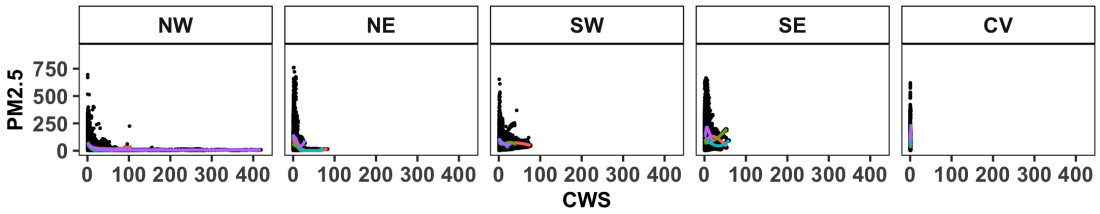

(b) Beijing NW

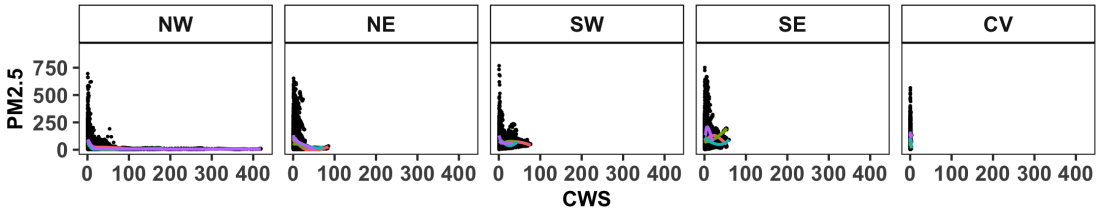

(c) Tangshan

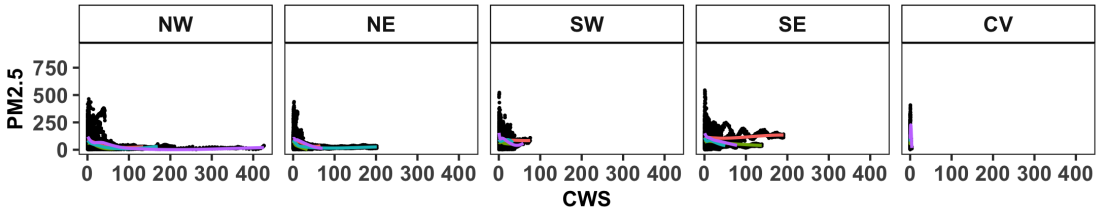

(d) Baoding

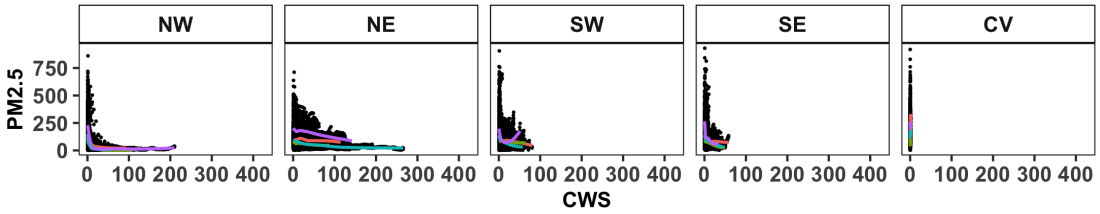

Figure S2: $PM_{2.5}$ ($\mu g/m^3$) versus the cumulated wind speed (CWS, m/s) under the five wind directions in the four site clusters from March 2015 to February 2016 with locally weighted scatterplot smoothing curves (solid lines) for spring (red), summer (green), autumn (blue) and winter (purple). The plots for other years were similar.

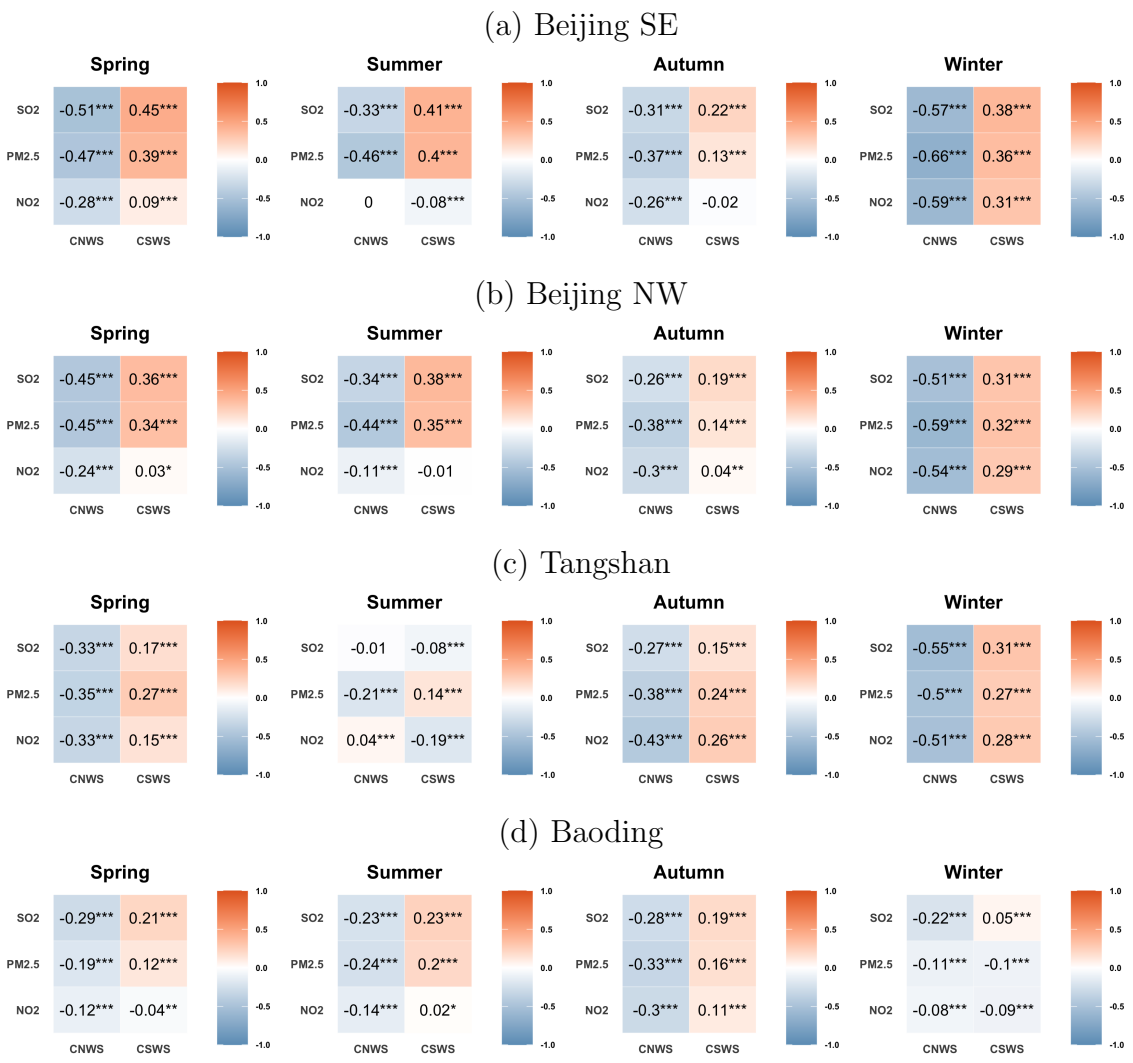

Figure S3: Pair-wise seasonal Spearman's rank correlation coefficients between the three pollutants ($PM_{2.5}$, SO_2 and NO_2, $\mu g/m^3$) and the cumulative northerly and southerly wind speeds (m/s) in 2015 for the four site clusters: (a) Beijng SE, (b) Beijng NW, (c) Tangshan and (d) Baoding. The number of * indicates the level of significance in the association (*: p-value<0.05; **: p-value < 0.01; ***: p-value < 0.001).

(a) Spring

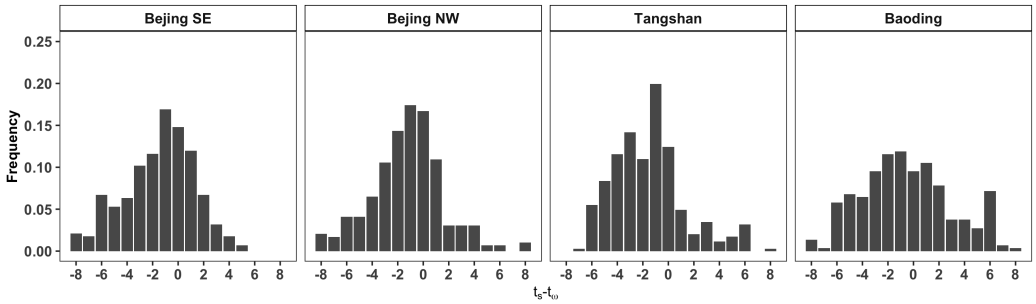

(b) Summer

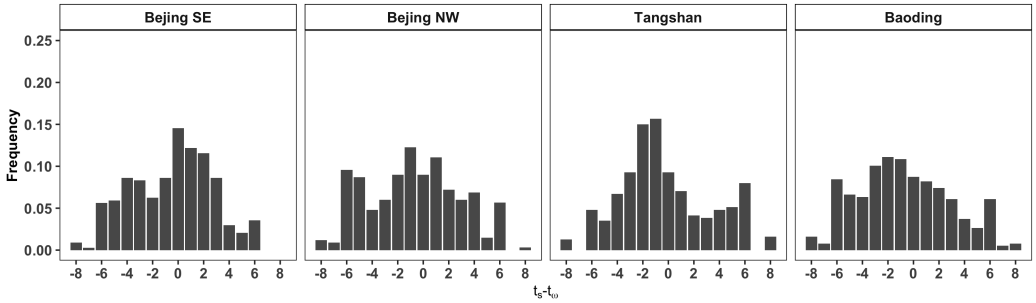

(c) Autumn

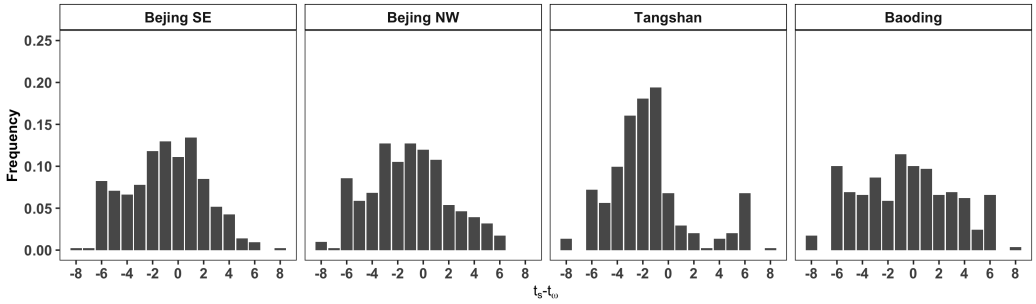

(d) Winter

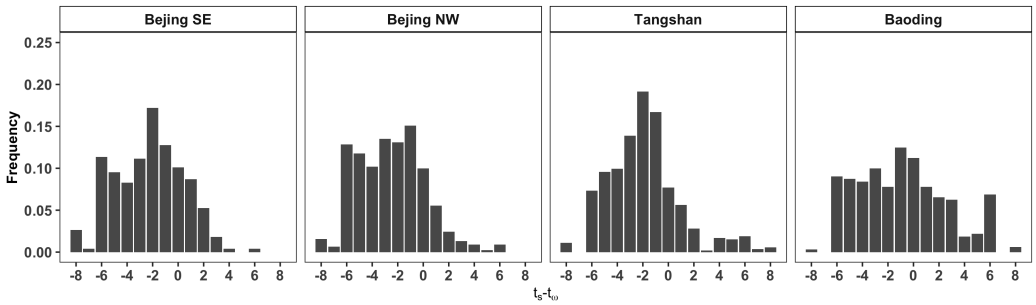

Figure S4: The histograms of the differences $t_s - t_\omega$ (hours) between the ending time t_ω of strong northerly cleaning processes and the starting time t_s of the selected calm episodes in different seasons for four clusters.

(a) $t_s < t_\omega$ (60.6%)

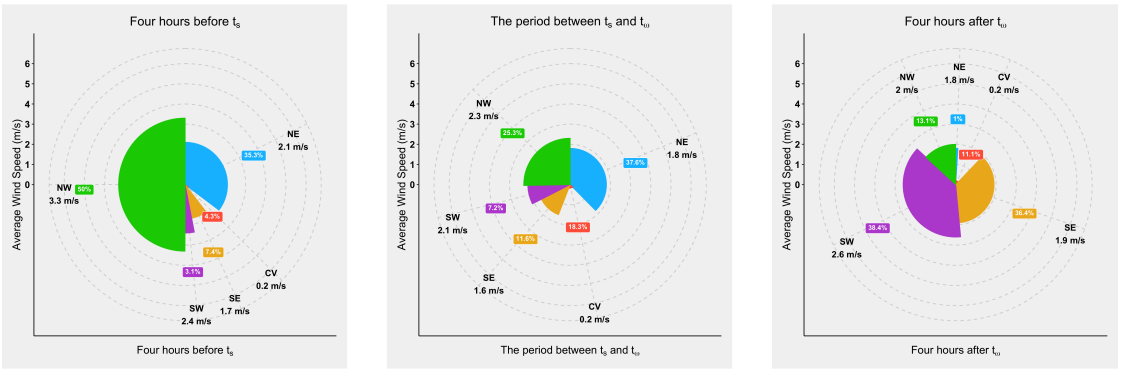

(b) $t_s = t_\omega$ (15.0%)

(c) $t_s > t_\omega$ (24.4%)

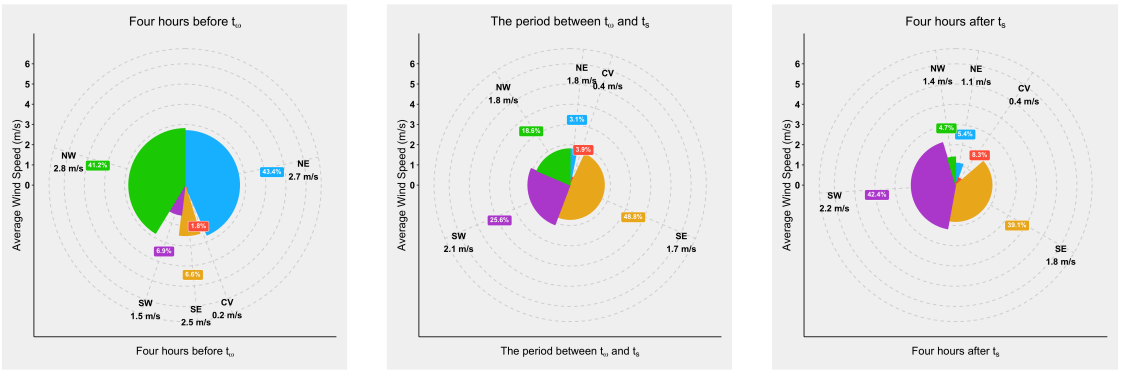

Figure S5: The distributions of five wind directions (via angle widths) and the average wind speed (via radius) for three periods (4 hours before $\min\{t_s, t_\omega\}$, between t_s and t_ω, and 4 hours after $\max\{t_s, t_\omega\}$) of selected calm episodes in the spring of Beijing SE: (a) the episode starts before the end of northerly cleaning, $t_s < t_\omega$, (b) the starting time of the episode equals to the end of northerly cleaning, $t_s = t_\omega$ and (c) the episode starts after the end of northerly cleaning $t_s > t_\omega$. The percentages of the three situations are given in the parentheses.

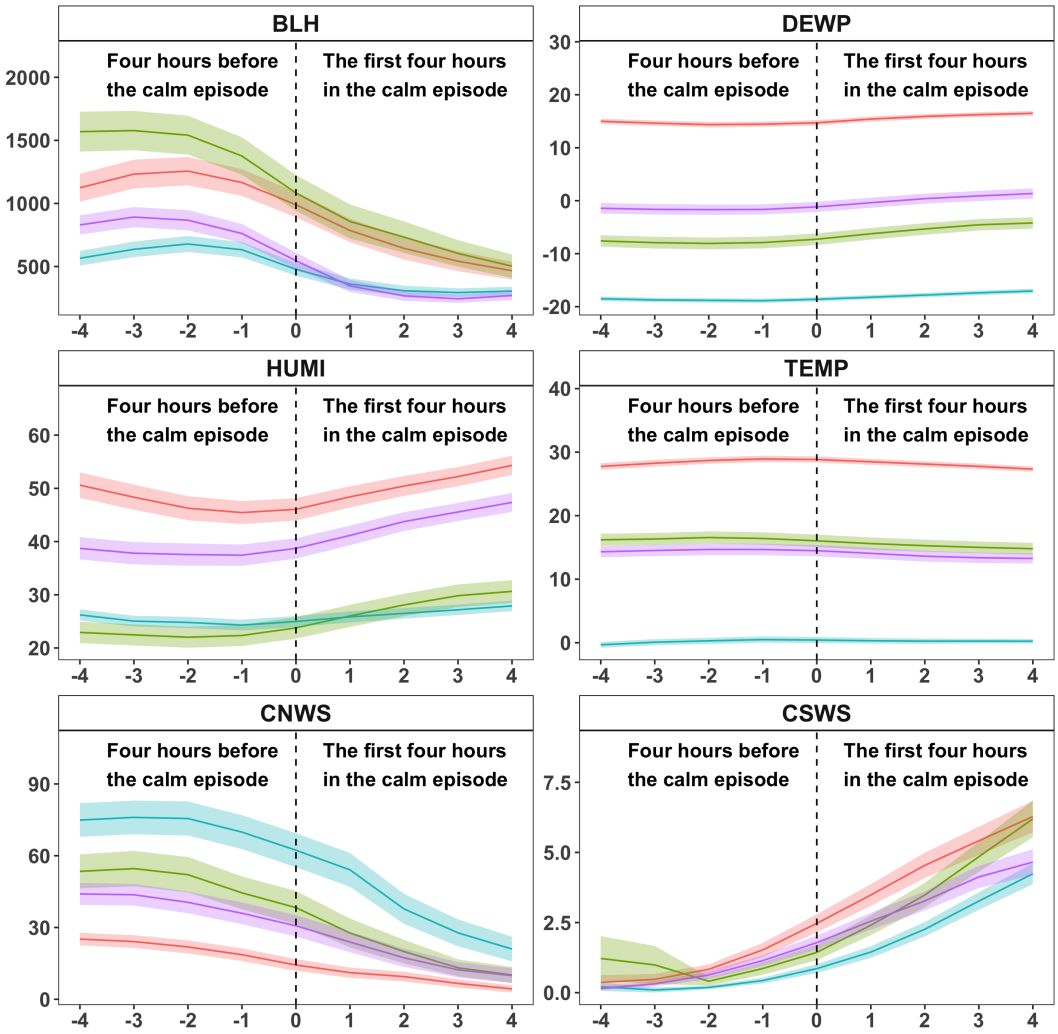

Figure S6: The average boundary layer height (BLH), dew point (DEWP), relative humidity (HUMI), temperature (TEMP), cumulative northerly wind speed (CNWS), and cumulative southerly wind speed (CSWS) in the four hours before and after the start of the calm episodes indicated by the dashed vertical line at zero in Beijing SE in spring (green), summer (red), autumn (purple) and winter (blue) with the 95% confidence intervals indicated by the colored areas.

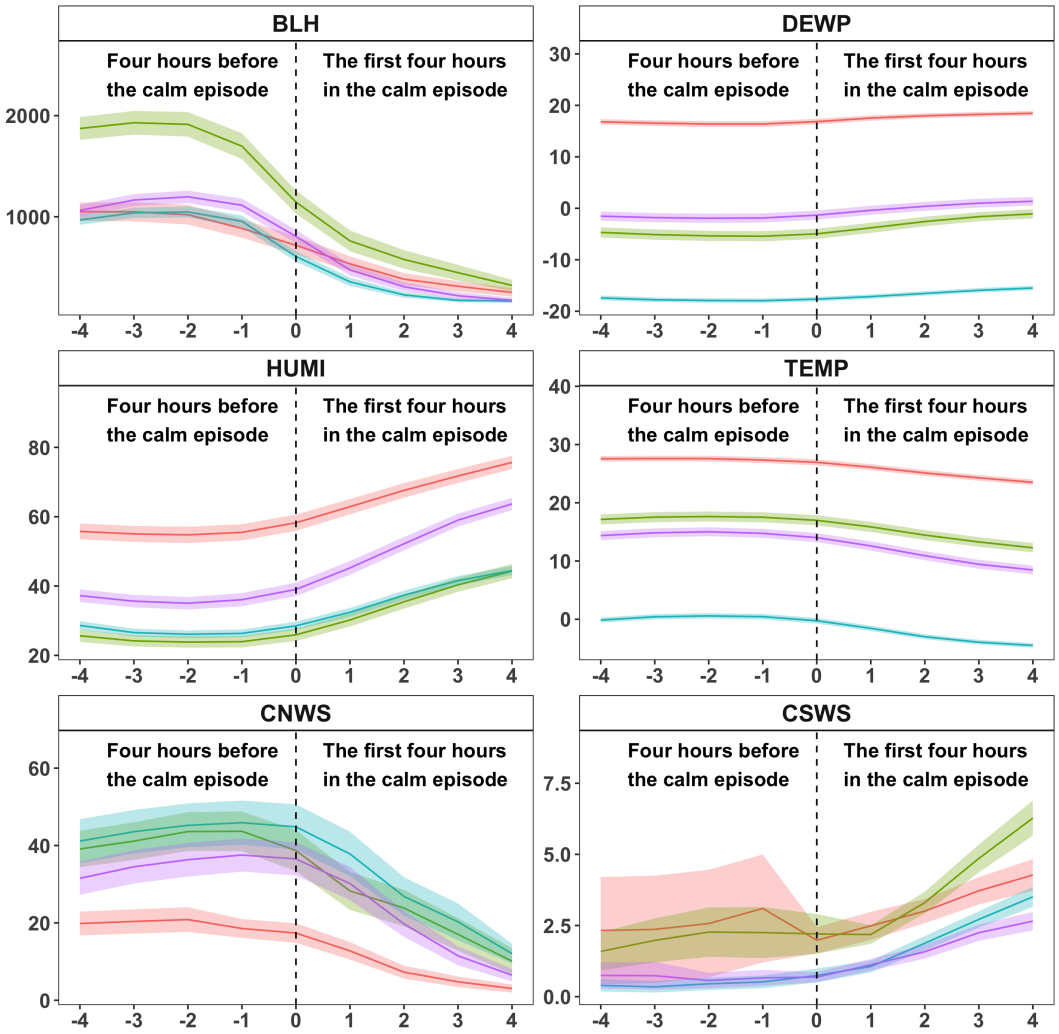

Figure S7: The average boundary layer height (BLH), dew point (DEWP), relative humidity (HUMI), temperature (TEMP), cumulative northerly wind speed (CNWS), and cumulative southerly wind speed (CSWS) in the four hours before and after the start of the calm episodes indicated by the dashed vertical line at zero in Tangshan in spring (green), summer (red), autumn (purple) and winter (blue) with the 95% confidence intervals indicated by the colored areas.

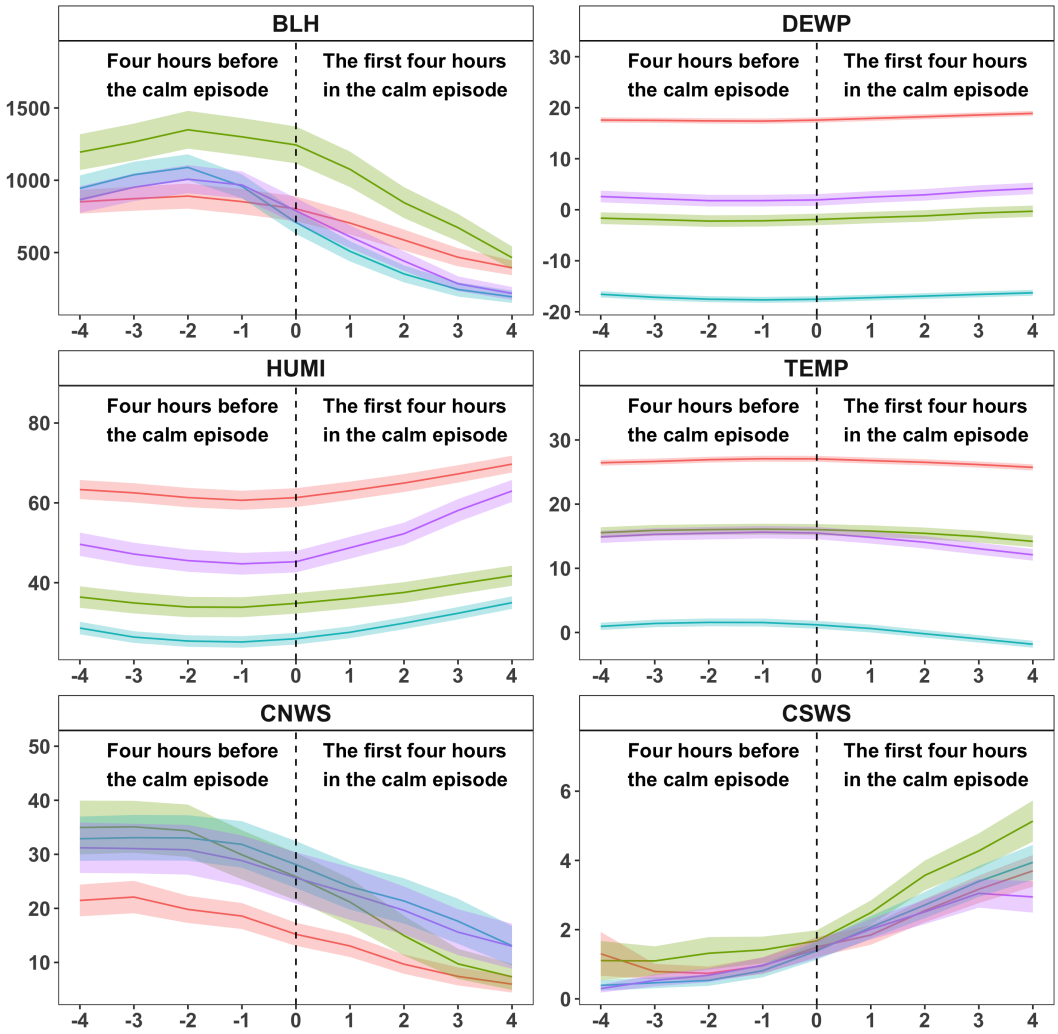

Figure S8: The average boundary layer height (BLH), dew point (DEWP), relative humidity (HUMI), temperature (TEMP), cumulative northerly wind speed (CNWS), and cumulative southerly wind speed (CSWS) in the four hours before and after the start of the calm episodes indicated by the dashed vertical line at zero in Baoding in spring (green), summer (red), autumn (purple) and winter (blue) with the 95% confidence intervals indicated by the colored areas.

(a) $PM_{2.5}$

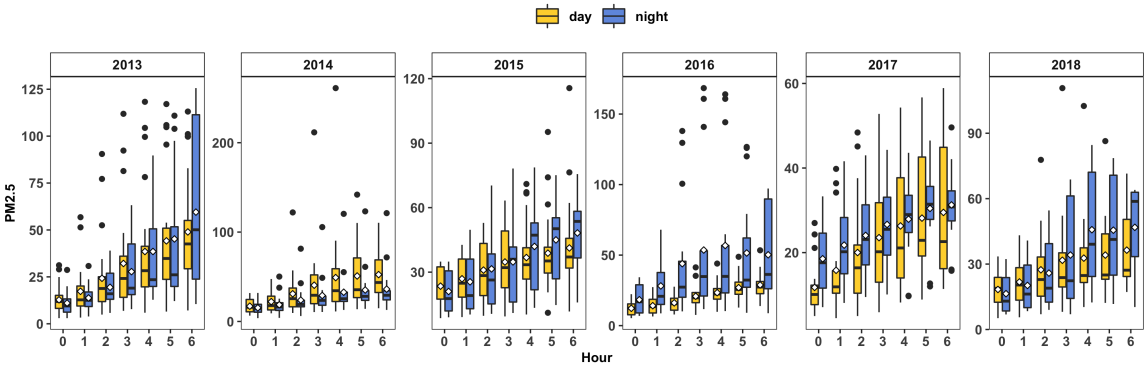

(b) NO_2

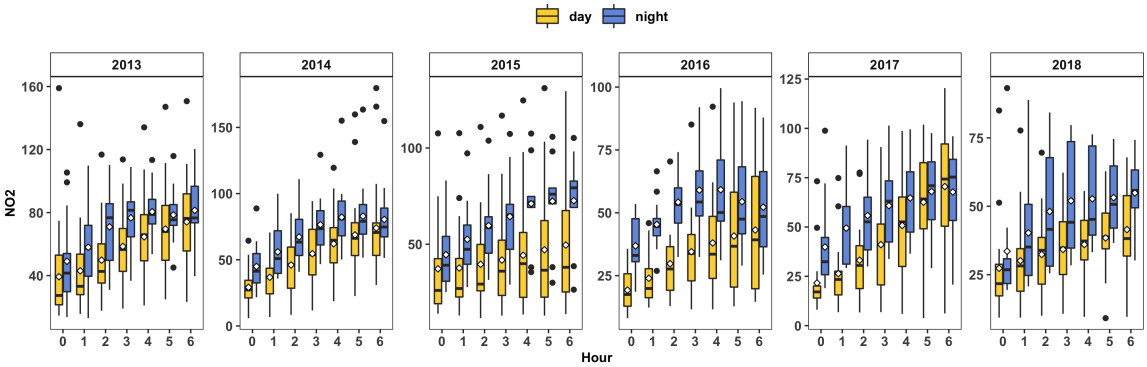

(c) SO_2

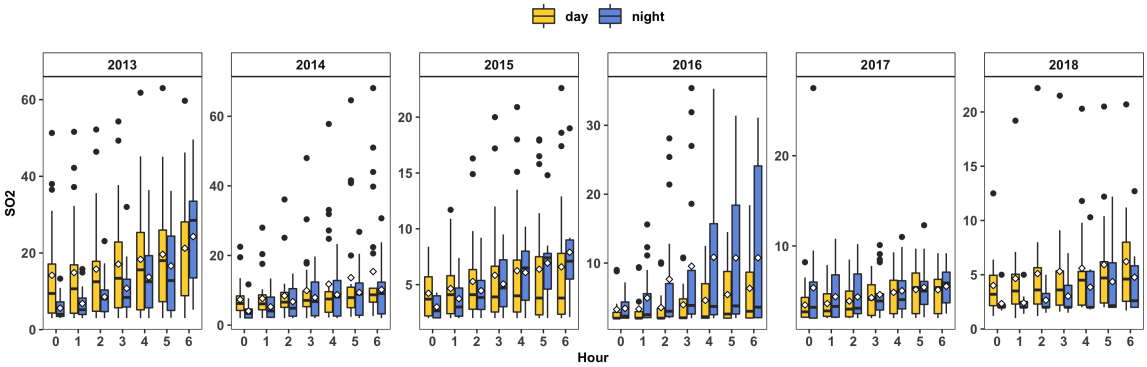

Figure S9: The boxplots of concentrations ($\mu g/m^3$) for (a) $PM_{2.5}$, (b) NO_2 and (c) SO_2 in the first six hours during the episodes in spring of cluster Beijing NW with the start point of episodes (hour 0 on the horizontal axis) in the day (6 am-6 pm, yellow) and night (7 pm-5 am, blue).

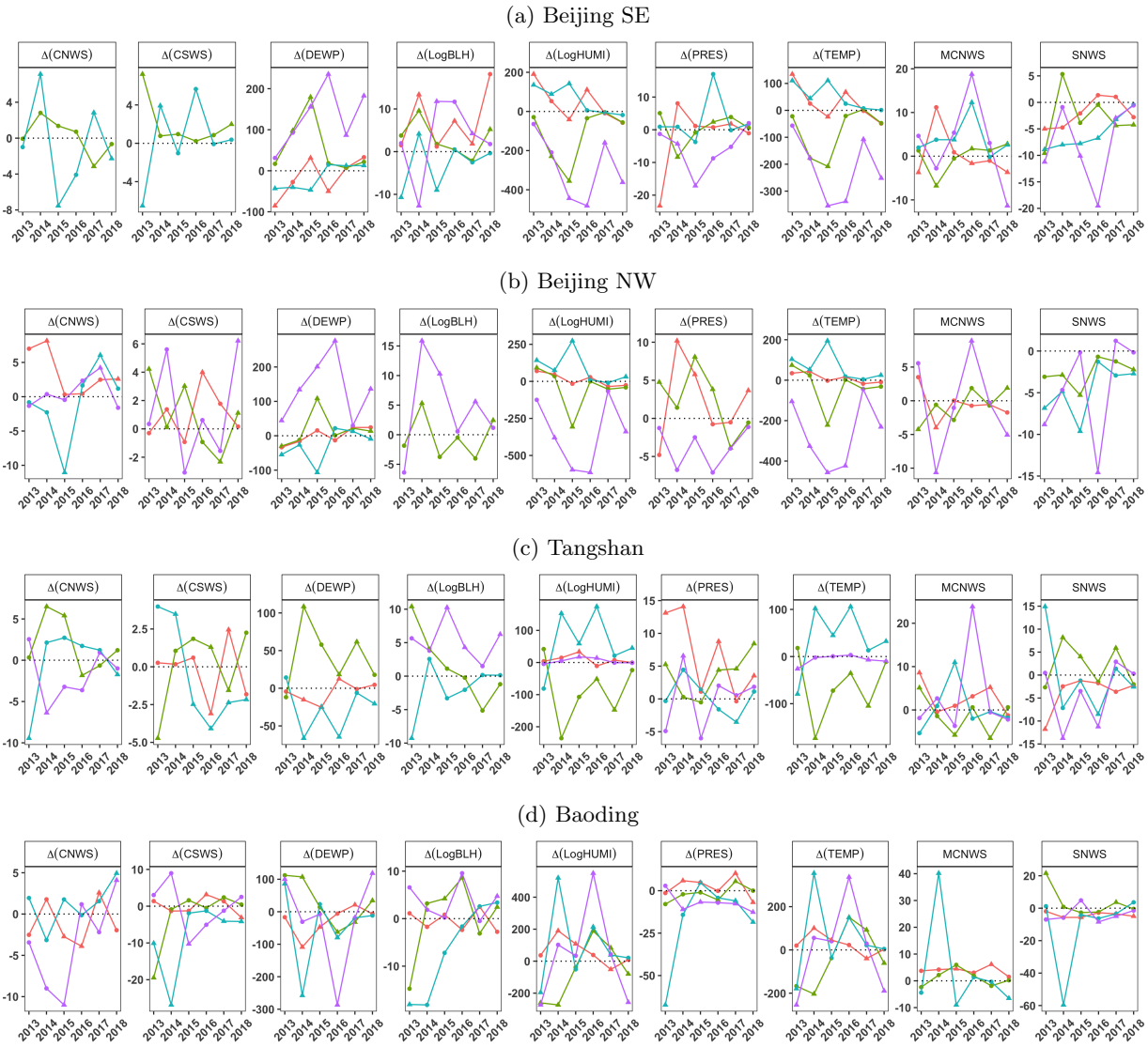

Figure S10: The estimates for coefficients of selected variables in models for $PM_{2.5}$ in the first six hours of calm episodes for cluster (a) Beijing SE, (b) Beijing NW, (c) Tangshan, (d) Baoding in spring (red), summer (green), autumn (blue) and winter (purple) of six seasonal years with significant and non-significant effects shown by points in the shape of triangle and circular, respectively. The dotted line represents zero.

(a) Beijing SE

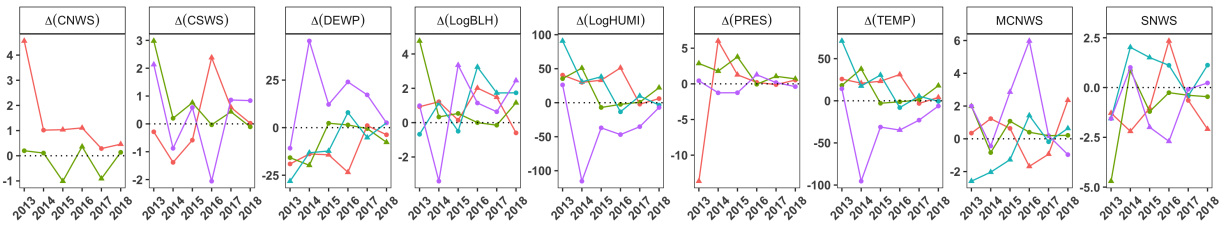

(b) Beijing NW

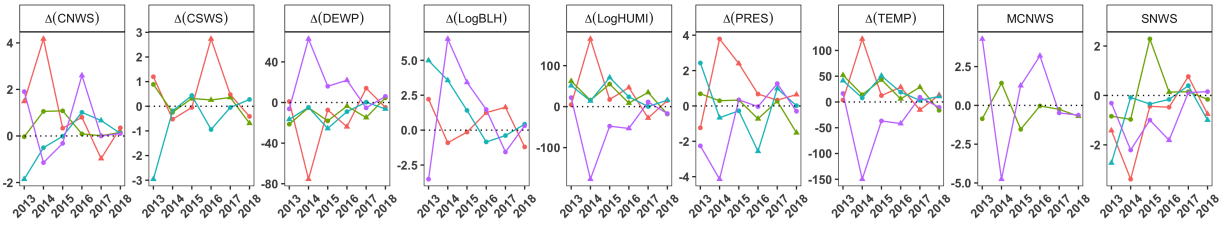

(c) Tangshan

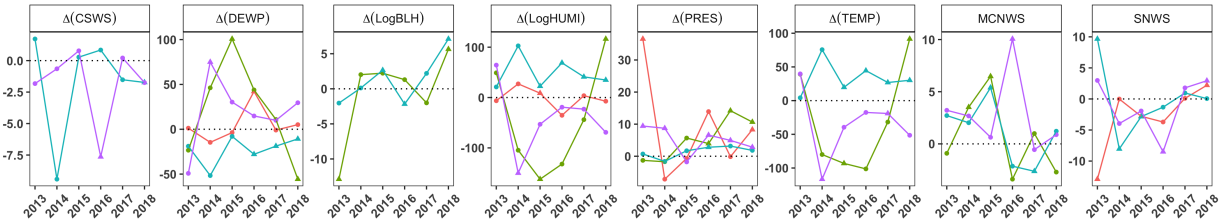

(d) Baoding

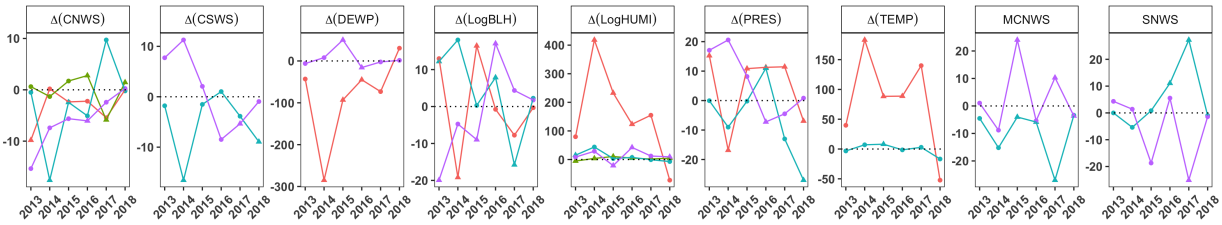

Figure S11: The estimates for coefficients of selected variables in models for SO_2 in the first six hours of calm episodes for cluster (a) Beijing SE, (b) Beijing NW, (c) Tangshan, (d) Baoding in spring (red), summer (green), autumn (blue) and winter (purple) of six seasonal years with significant and non-significant effects shown by points in the shape of triangle and circular, respectively. The dotted line represents zero.

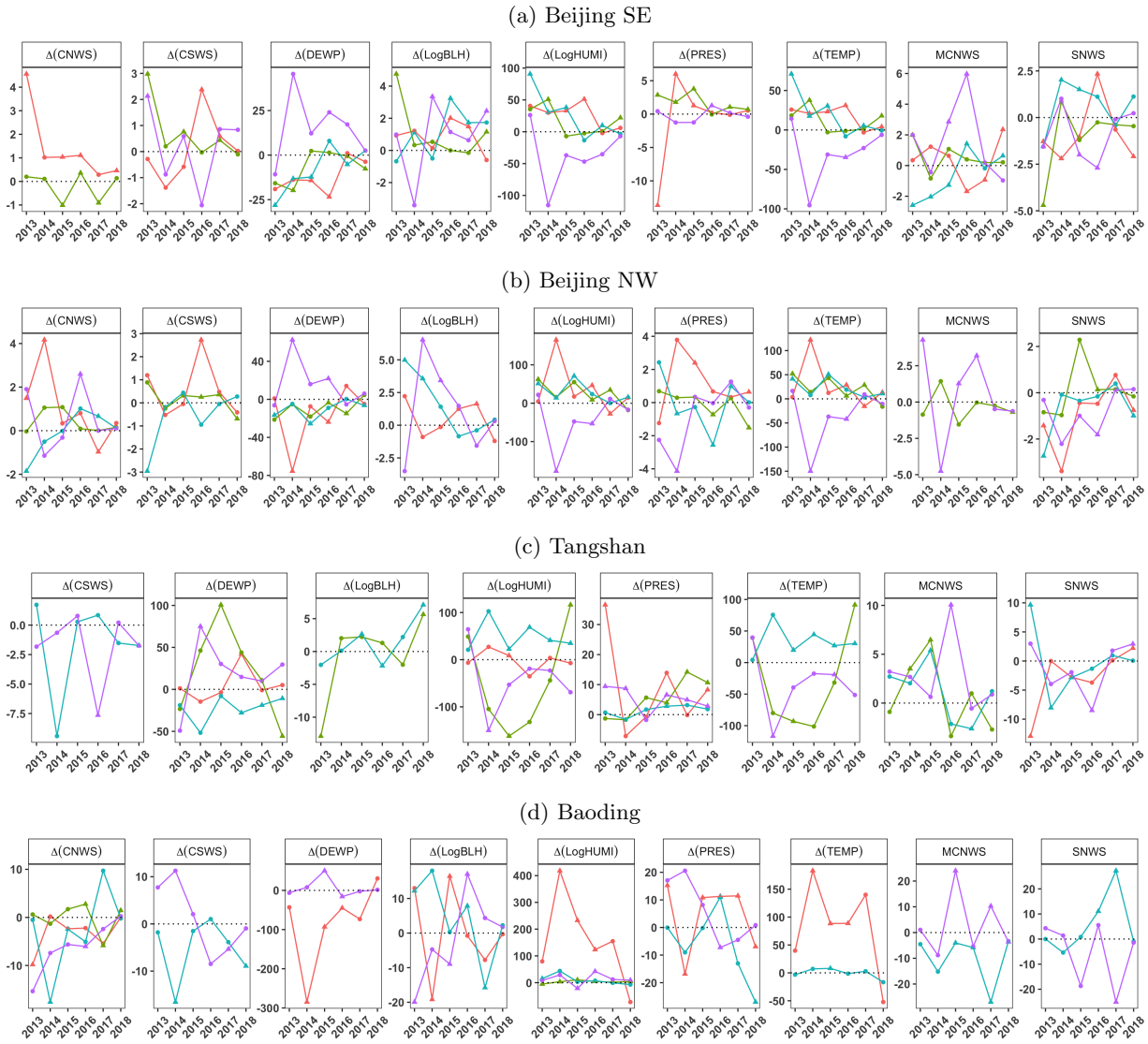

Figure S12: The estimates for coefficients of selected variables in models for NO_2 in the six seven hours of calm episodes for cluster (a) Beijing SE, (b) Beijing NW, (c) Tangshan, (d) Baoding in spring (red), summer (green), autumn (blue) and winter (purple) of six seasonal years with significant and non-significant effects shown by points in the shape of triangle and circular, respectively. The dotted line represents zero.

(a) Spring

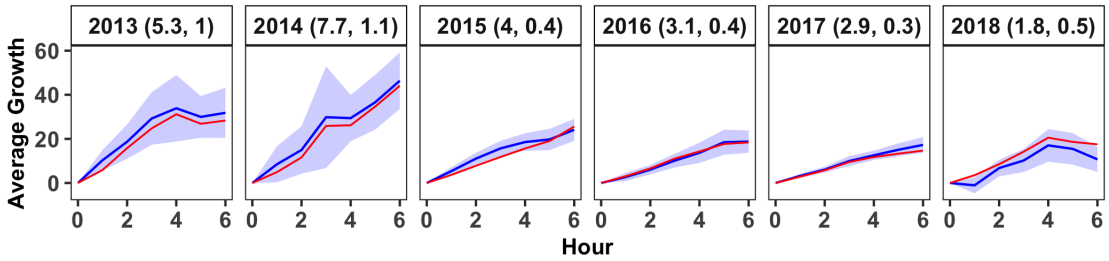

(b) Summer

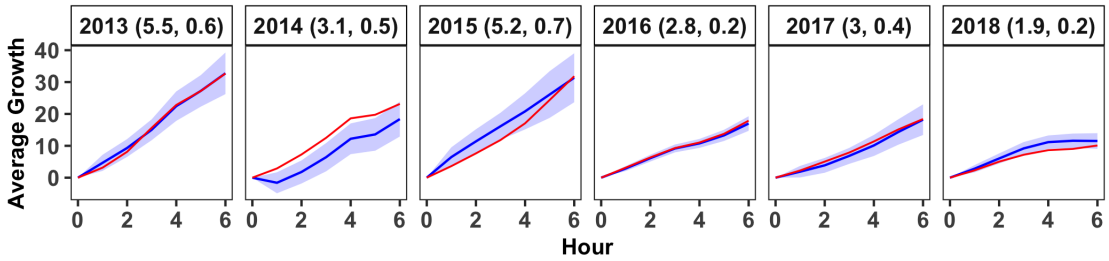

(c) Autumn

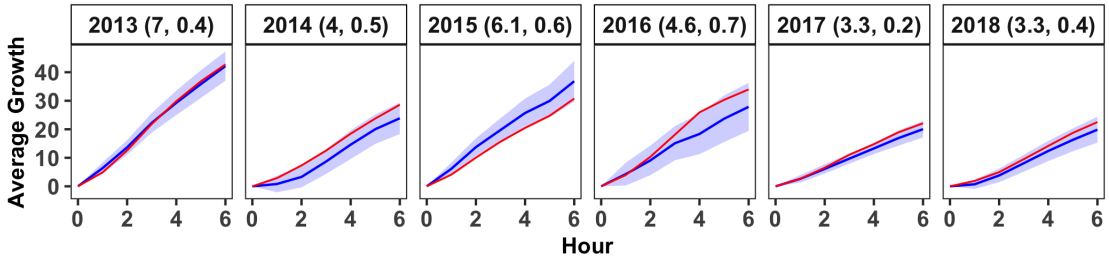

(d) Winter

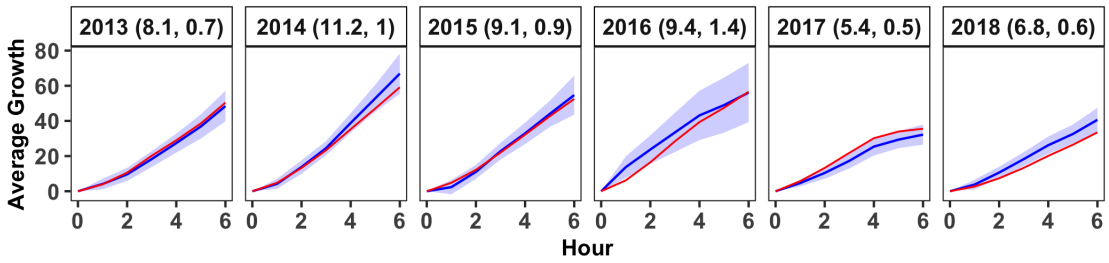

Figure S13: The adjusted (blue) and original (red) average growth ($\mu g/m^3$) of $PM_{2.5}$ in the first six hours of the calm episode for cluster Beijing SE in (a) spring (b) summer (c) autumn and (d) winter of six years. The 95% confidence intervals of adjusted averaged change of $PM_{2.5}$ are indicated by shading. And the adjusted average growth rates ($\mu g/m^3$ per hour) in the first six hours of the episodes with the standard errors are marked in the parentheses.

(a) Spring

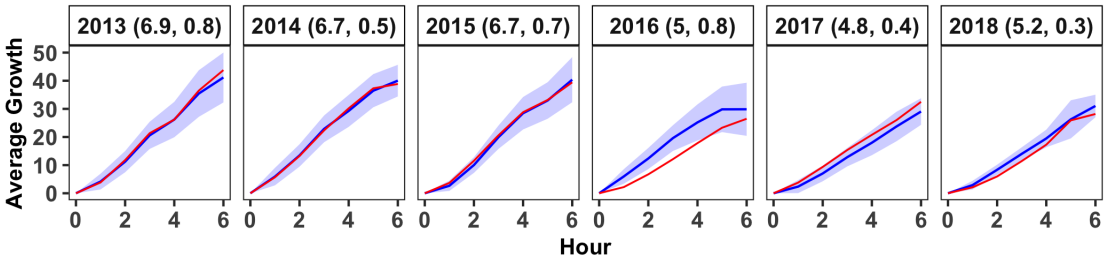

(b) Summer

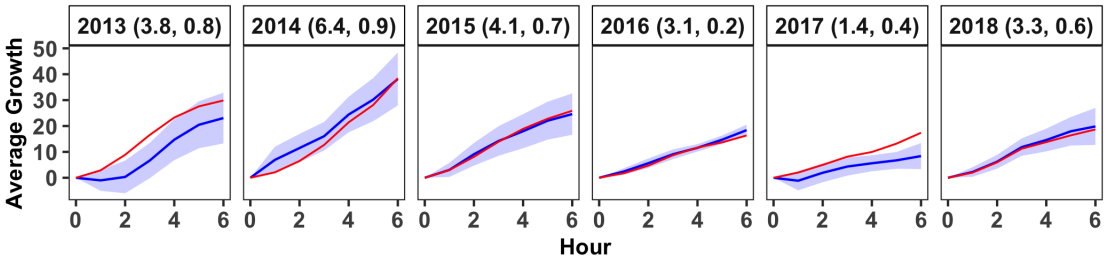

(c) Autumn

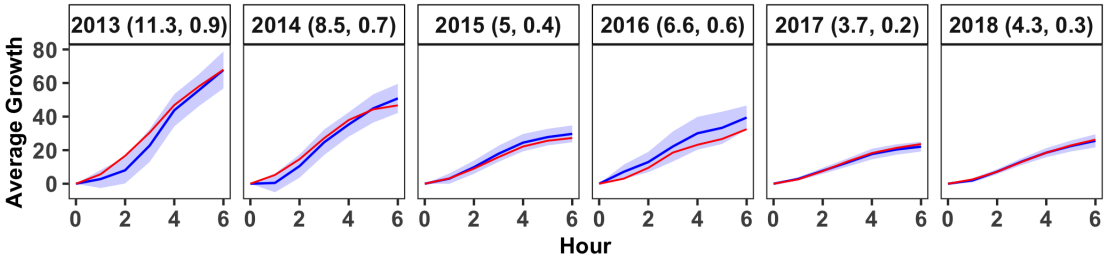

(d) Winter

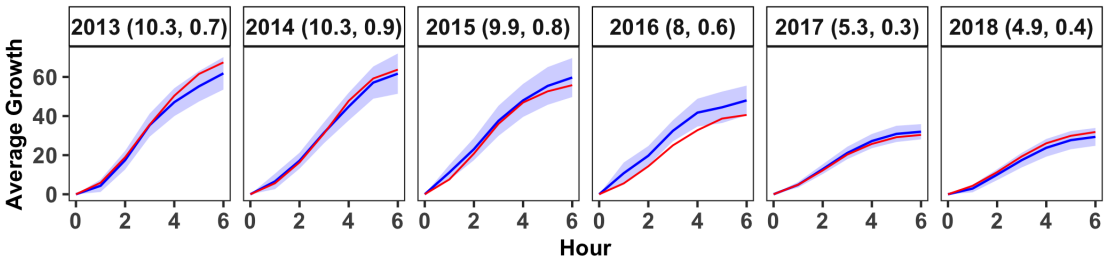

Figure S14: The adjusted (blue) and original (red) average growth ($\mu g/m^3$) of $PM_{2.5}$ in the first six hours of the calm episode for cluster in Tangshan in (a) spring (b) summer (c) autumn and (d) winter of six years. The 95% confidence intervals of adjusted averaged change of $PM_{2.5}$ are indicated by shading. And the adjusted average growth rates ($\mu g/m^3$ per hour) in the first six hours of the episodes with the standard errors are marked in the parentheses.

(a) Spring

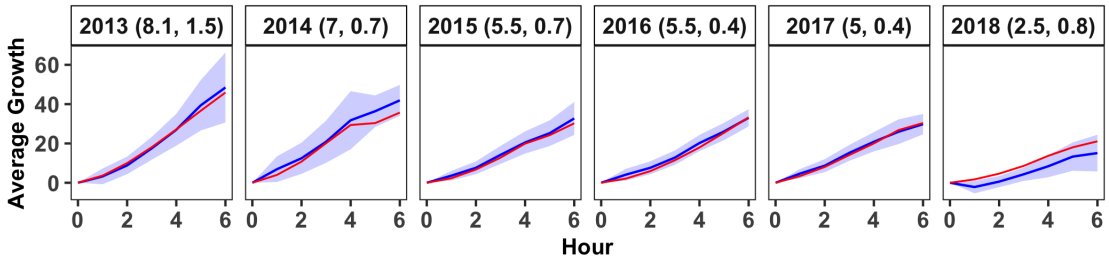

(b) Summer

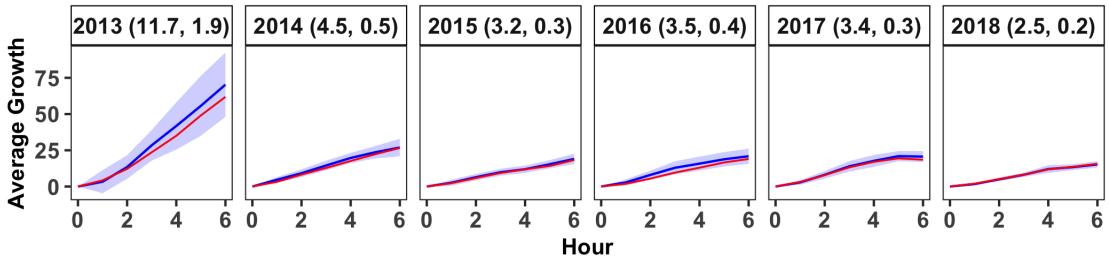

(c) Autumn

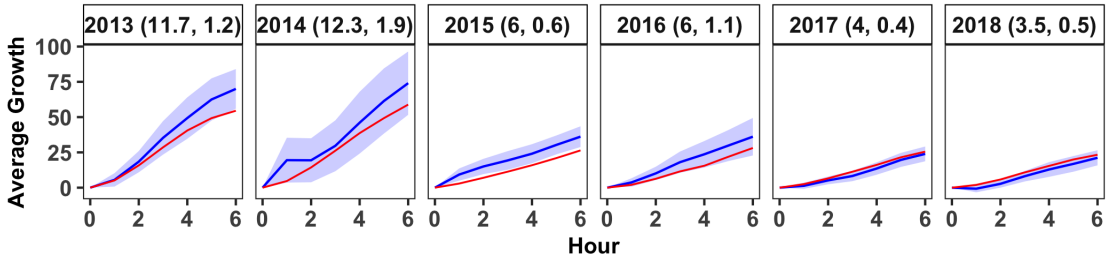

(d) Winter

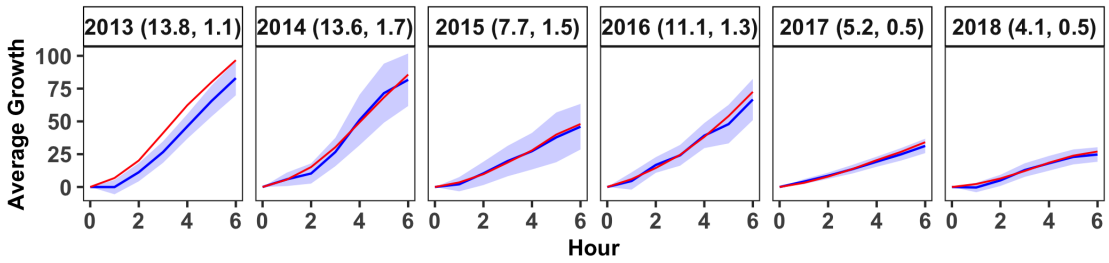

Figure S15: The adjusted (blue) and original (red) average growth ($\mu g/m^3$) of $PM_{2.5}$ in the first six hours of the calm episode for cluster in Baoding in (a) spring (b) summer (c) autumn and (d) winter of six years. The 95% confidence intervals of adjusted averaged change of $PM_{2.5}$ are indicated by shading. And the adjusted average growth rates ($\mu g/m^3$ per hour) in the first six hours of the episodes with the standard errors are marked in the parentheses.

(a) Spring

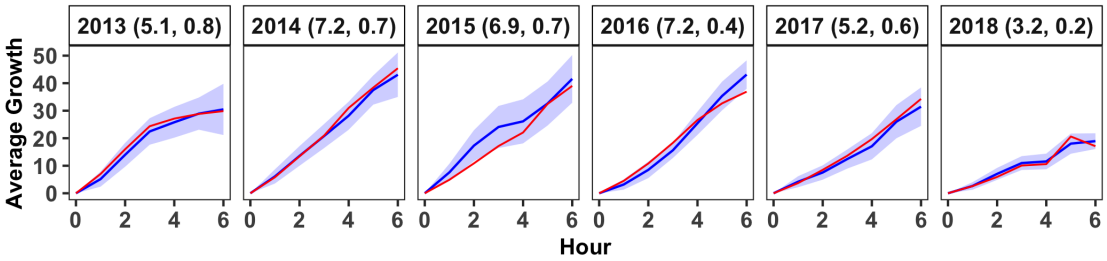

(b) Summer

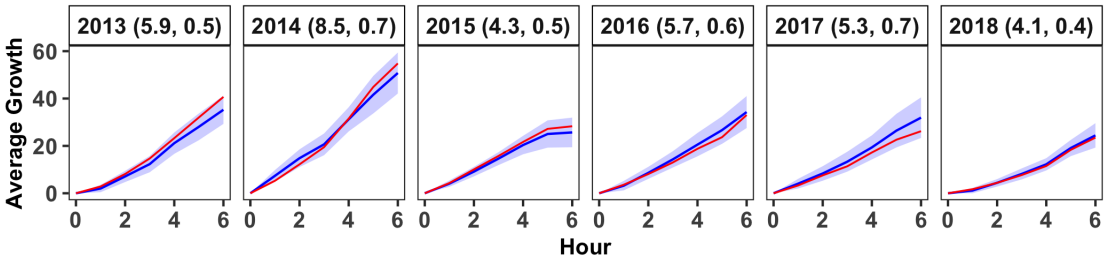

(c) Autumn

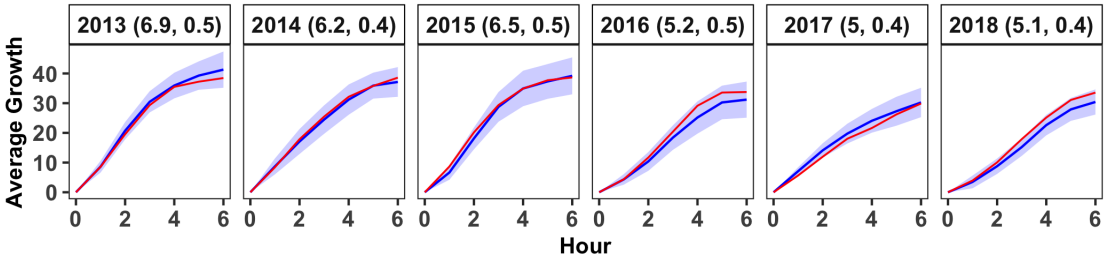

(d) Winter

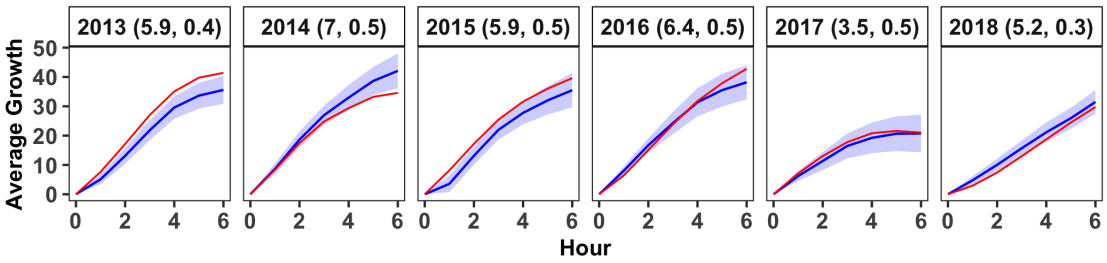

Figure S16: The adjusted (blue) and original (red) average growth ($\mu g/m^3$) of NO_2 in the first six hours of the calm episode for cluster Beijing SE in (a) spring (b) summer (c) autumn and (d) winter of six years. The 95% confidence intervals of adjusted averaged change of NO_2 are indicated by shading. And the adjusted average growth rates ($\mu g/m^3$ per hour) in the first six hours of the episodes with the standard errors are marked in the parentheses.

(a) Spring

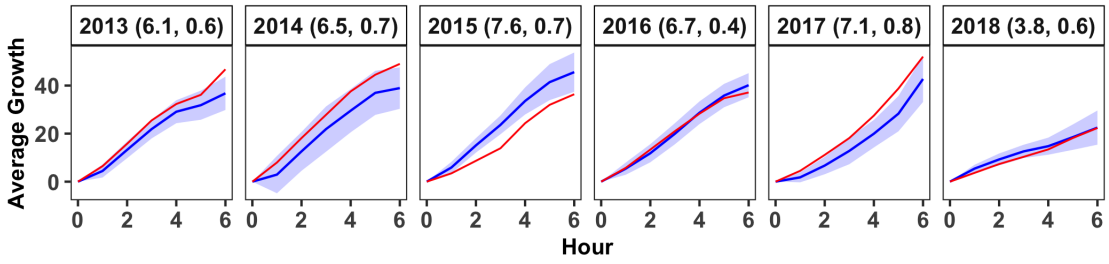

(b) Summer

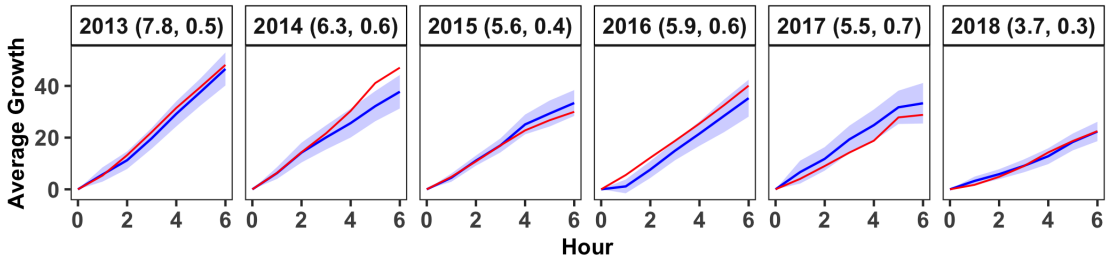

(c) Autumn

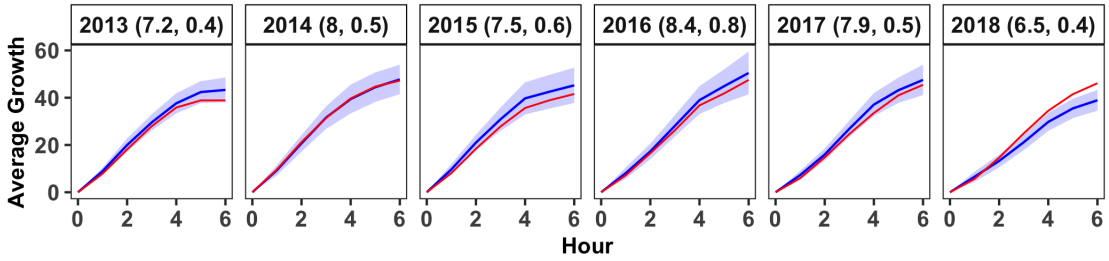

(d) Winter

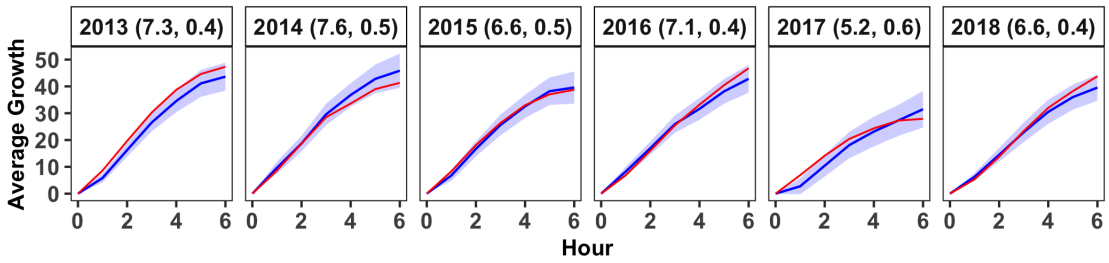

Figure S17: The adjusted (blue) and original (red) average growth (μg/m^3) of NO_2 in the first six hours of the calm episode for cluster Beijing NW in (a) spring (b) summer (c) autumn and (d) winter of six years. The 95% confidence intervals of adjusted averaged change of NO_2 are indicated by shading. And the adjusted average growth rates (μg/m^3 per hour) in the first six hours of the episodes with the standard errors are marked in the parentheses.

(a) Spring

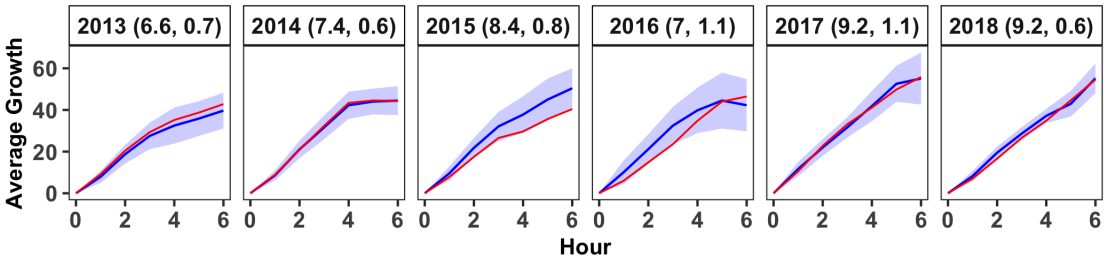

(b) Summer

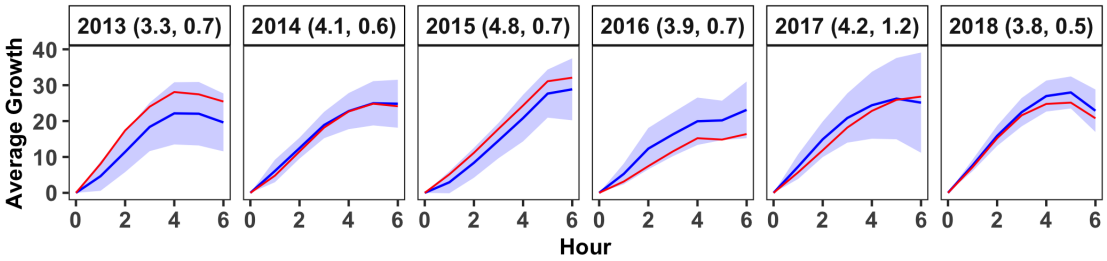

(c) Autumn

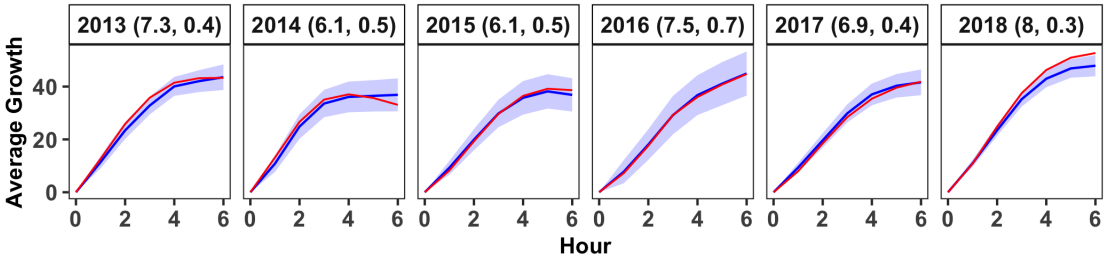

(d) Winter

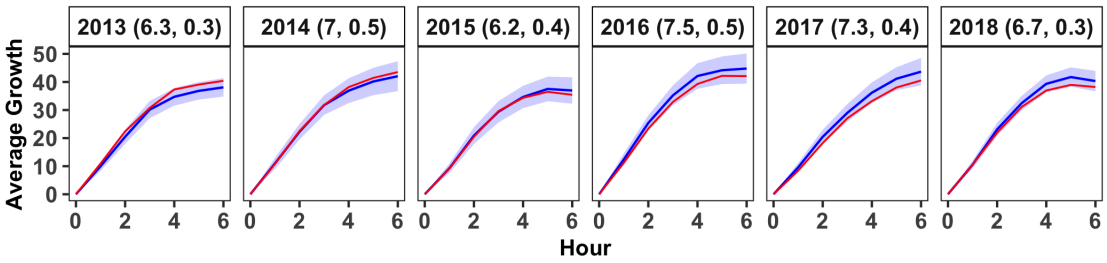

Figure S18: The adjusted (blue) and original (red) average growth ($\mu g/m^3$) of NO_2 in the first six hours of the calm episode for cluster in Tangshan in (a) spring (b) summer (c) autumn and (d) winter of six years. The 95% confidence intervals of adjusted averaged change of NO_2 are indicated by shading. And the adjusted average growth rates ($\mu g/m^3$ per hour) in the first six hours of the episodes with the standard errors are marked in the parentheses.

(a) Spring

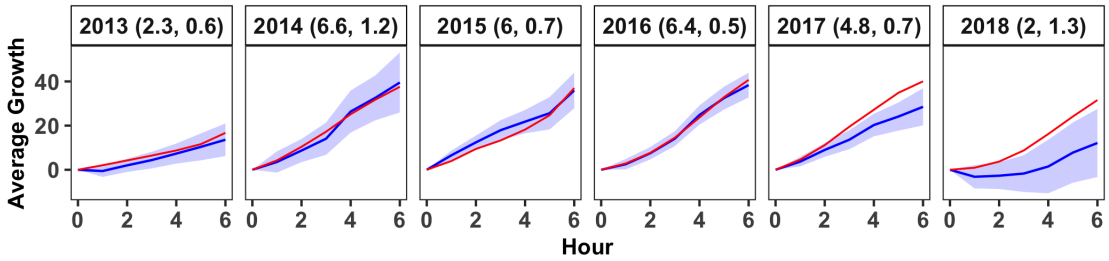

(b) Summer

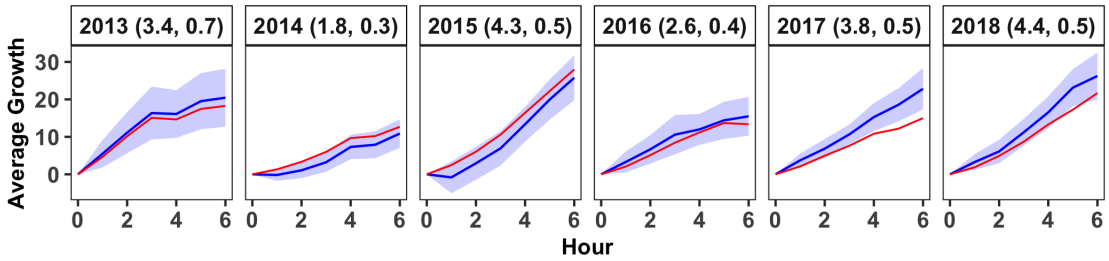

(c) Autumn

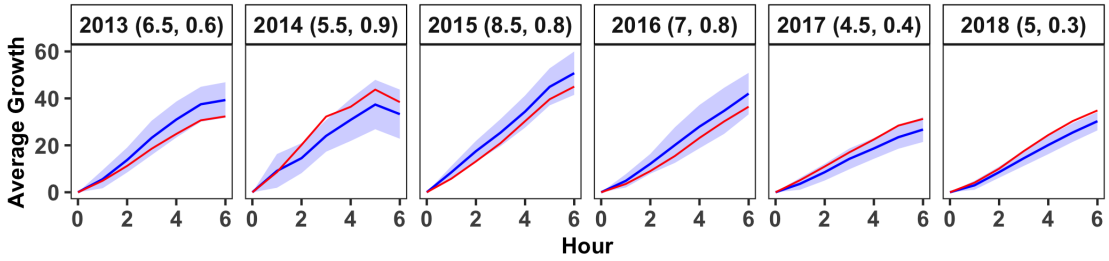

(d) Winter

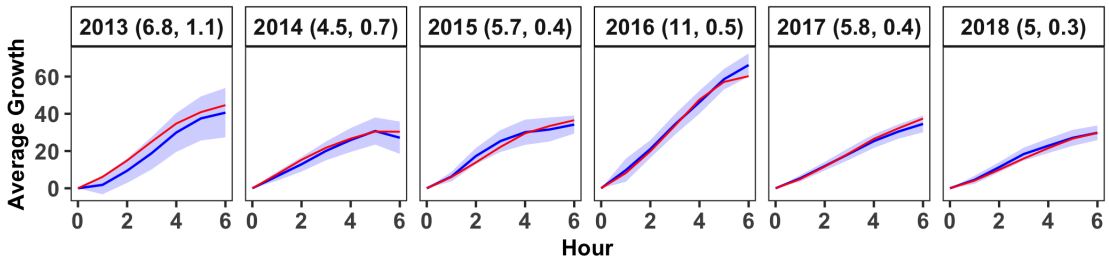

Figure S19: The adjusted (blue) and original (red) average growth (μg/m^3) of NO_2 in the first six hours of the calm episode for cluster in Baoding in (a) spring (b) summer (c) autumn and (d) winter of six years. The 95% confidence intervals of adjusted averaged change of NO_2 are indicated by shading. And the adjusted average growth rates (μg/m^3 per hour) in the first six hours of the episodes with the standard errors are marked in the parentheses.

(a) Spring

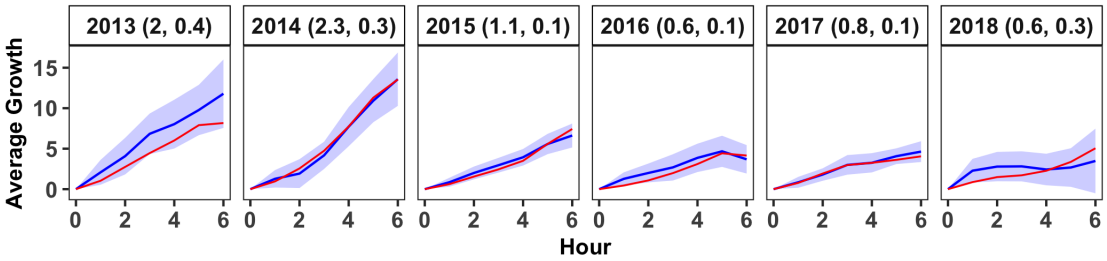

(b) Summer

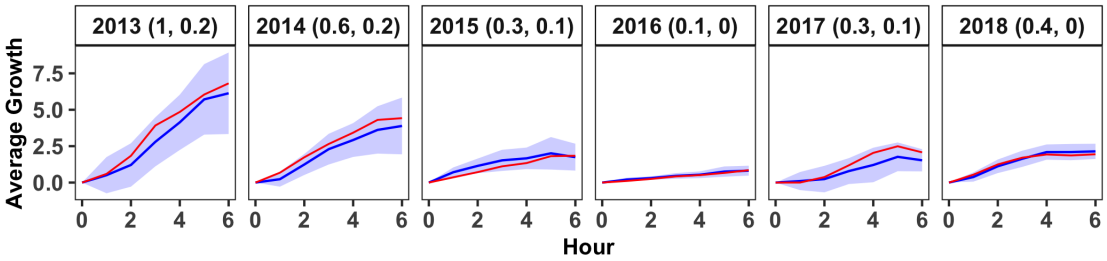

(c) Autumn

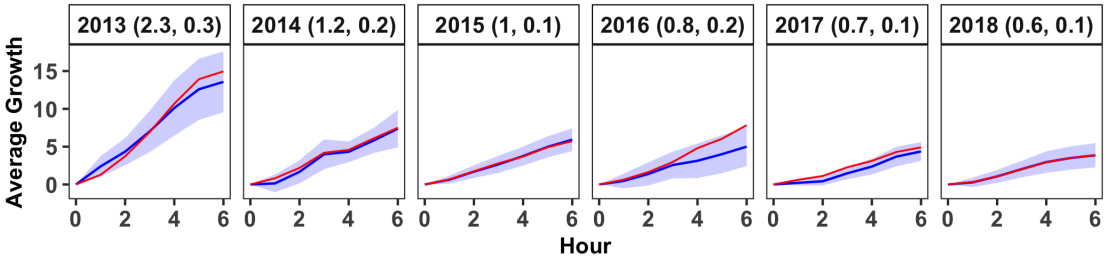

(d) Winter

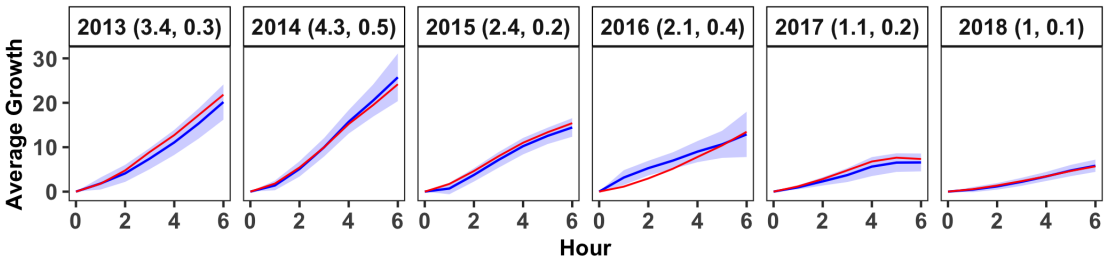

Figure S20: The adjusted (blue) and original (red) average growth ($\mu g/m^3$) of SO_2 in the first six hours of the calm episode for cluster Beijing SE in (a) spring (b) summer (c) autumn and (d) winter of six years. The 95% confidence intervals of adjusted averaged change of SO_2 are indicated by shading. And the adjusted average growth rates ($\mu g/m^3$ per hour) in the first six hours of the episodes with the standard errors are marked in the parentheses.

(a) Spring

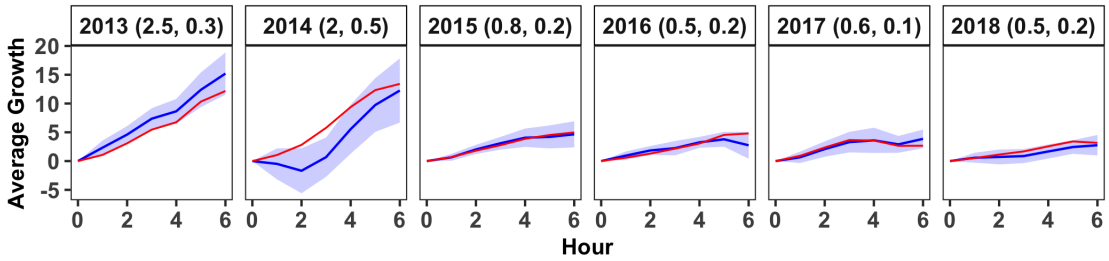

(b) Summer

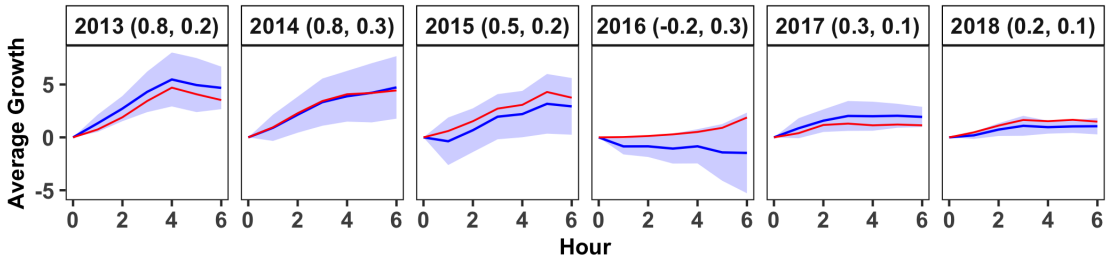

(c) Autumn

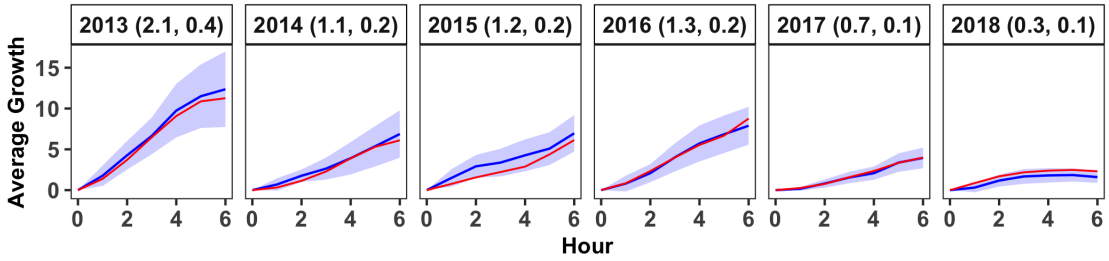

(d) Winter

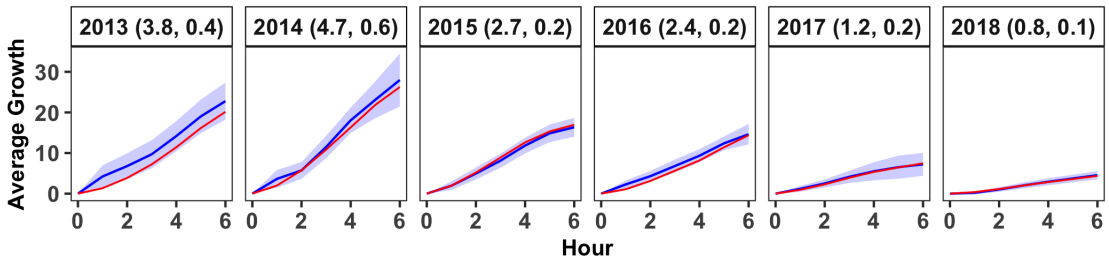

Figure S21: The adjusted (blue) and original (red) average growth ($\mu g/m^3$) of SO_2 in the first six hours of the calm episode for cluster Beijing NW in (a) spring (b) summer (c) autumn and (d) winter of six years. The 95% confidence intervals of adjusted averaged change of SO_2 are indicated by shading. And the adjusted average growth rates ($\mu g/m^3$ per hour) in the first six hours of the episodes with the standard errors are marked in the parentheses.

(a) Spring

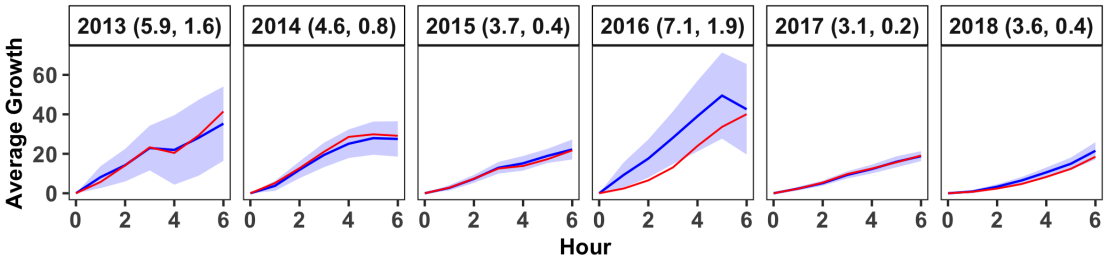

(b) Summer

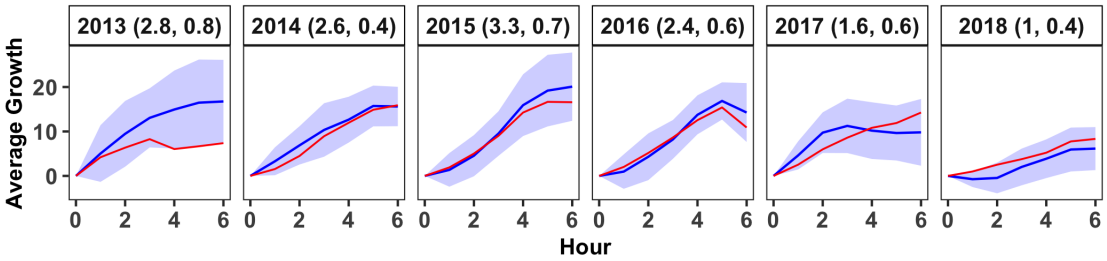

(c) Autumn

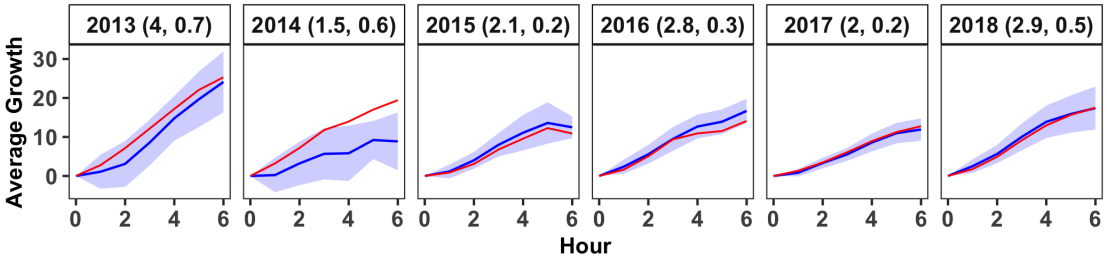

(d) Winter

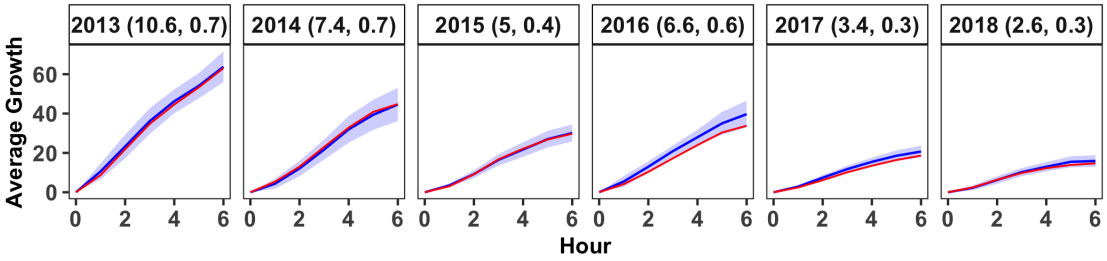

Figure S22: The adjusted (blue) and original (red) average growth ($\mu g/m^3$) of SO_2 in the first six hours of the calm episode for cluster in Tangshan in (a) spring (b) summer (c) autumn and (d) winter of six years. The 95% confidence intervals of adjusted averaged change of SO_2 are indicated by shading. And the adjusted average growth rates ($\mu g/m^3$ per hour) in the first six hours of the episodes with the standard errors are marked in the parentheses.

(a) Spring

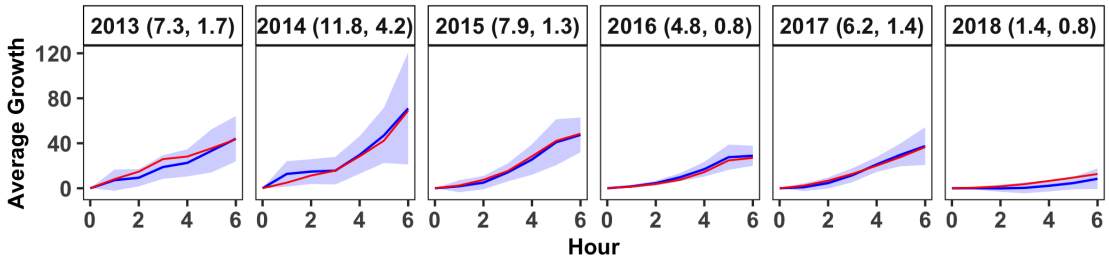

(b) Summer

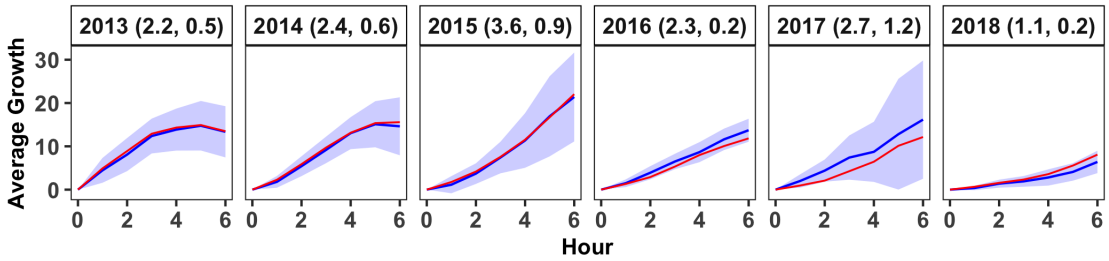

(c) Autumn

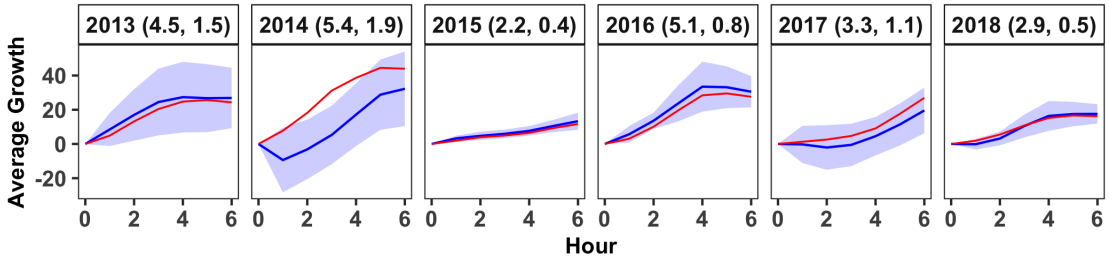

(d) Winter

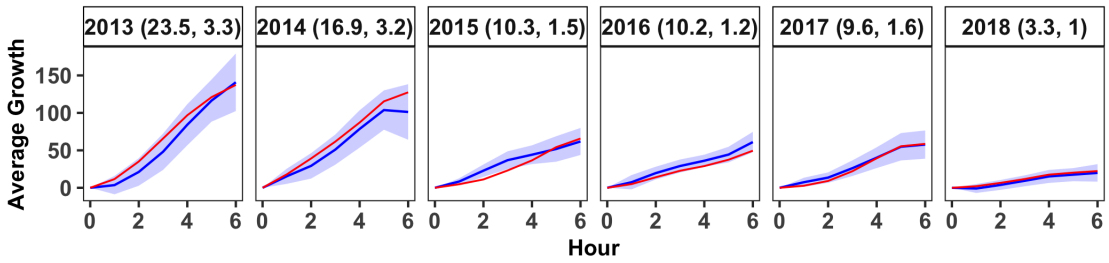

Figure S23: The adjusted (blue) and original (red) average growth ($\mu g/m^3$) of SO_2 in the first six hours of the calm episode for cluster in Baoding in (a) spring (b) summer (c) autumn and (d) winter of six years. The 95% confidence intervals of adjusted averaged change of SO_2 are indicated by shading. And the adjusted average growth rates ($\mu g/m^3$ per hour) in the first six hours of the episodes with the standard errors are marked in the parentheses.

(a) Total energy consumption

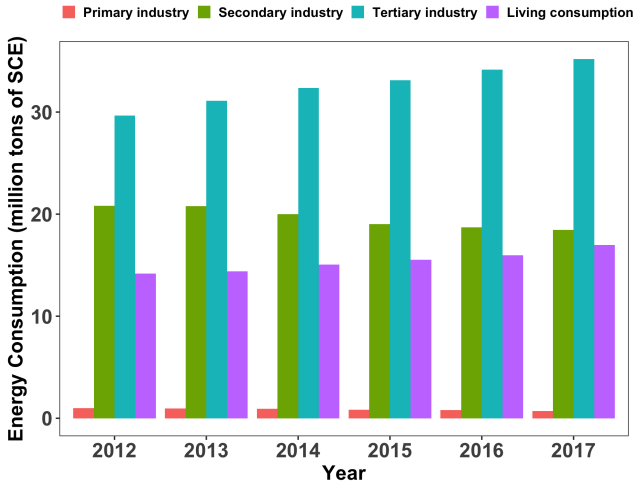

(b) Composition of energy consumption

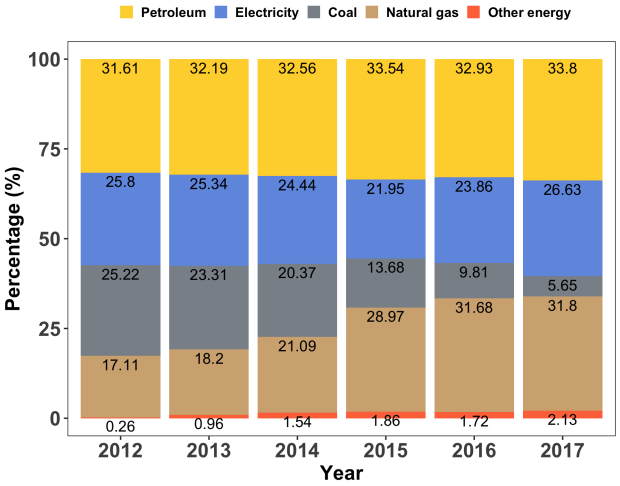

(c) NO_x emissions

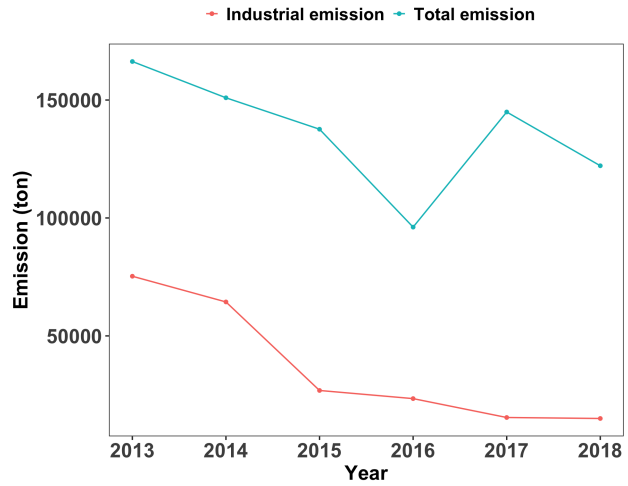

(d) SO_2 emissions

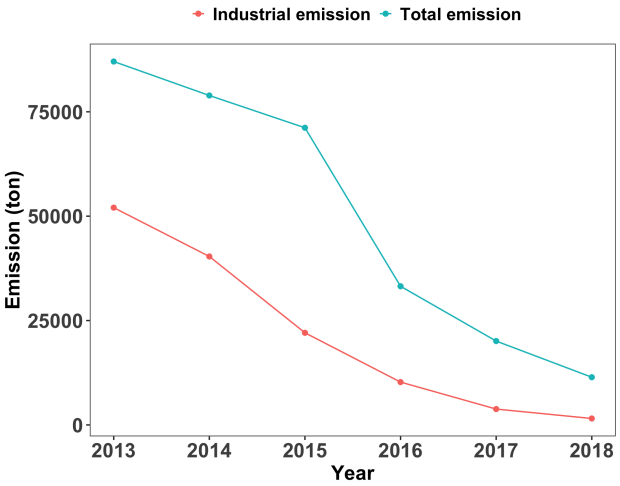

Figure S24: The (a) total energy consumption, (b) composition of energy consumption from 2012 to 2017, (c) nitrogen oxides emissions and (d) SO_2 emissions from 2013 to 2018 in Beijing.

(a) Output of main industrial products

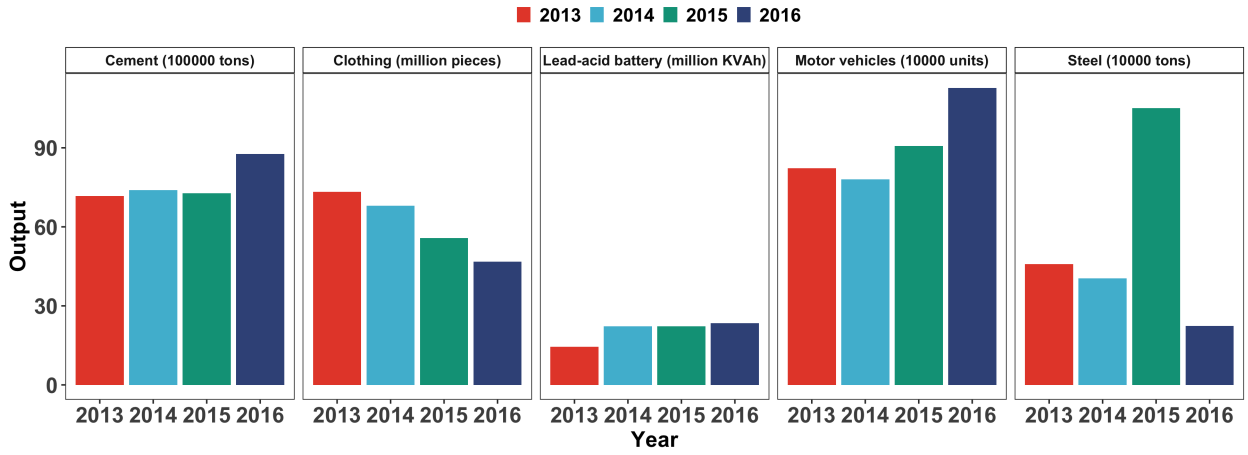

(b) Coal consumption

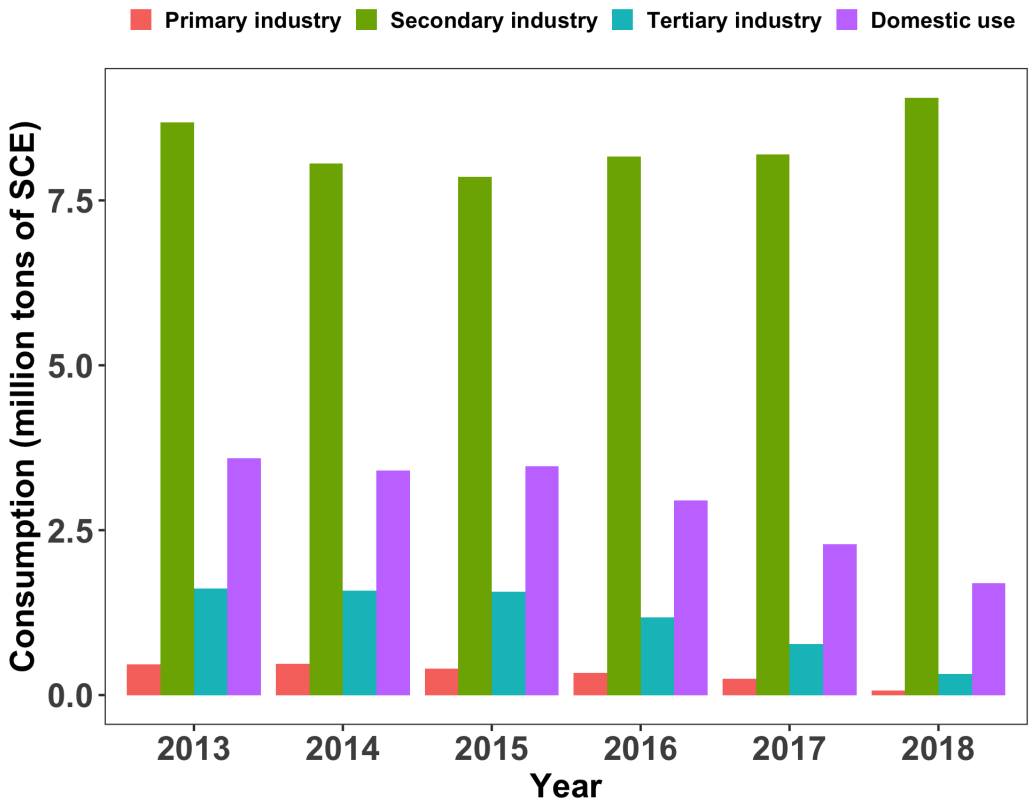

Figure S25: (a) Outputs of main industrial products from 2013 to 2016 and (b) coal consumptions from 2013 to 2018 in Baoding.

(a) Output of main heavy industrial products

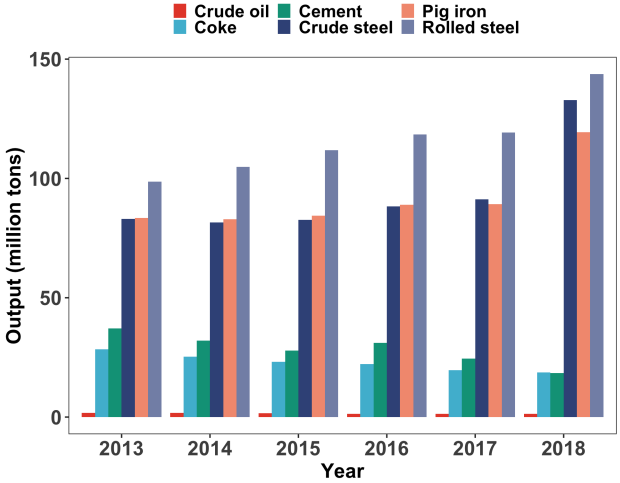

(b) SO_2 emissions

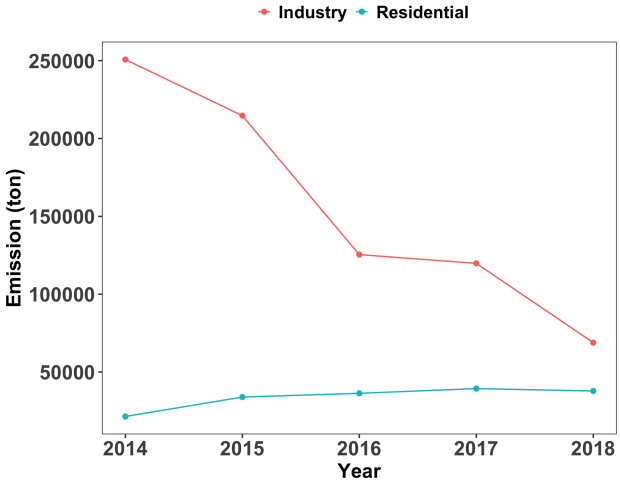

(c) NO_x emissions

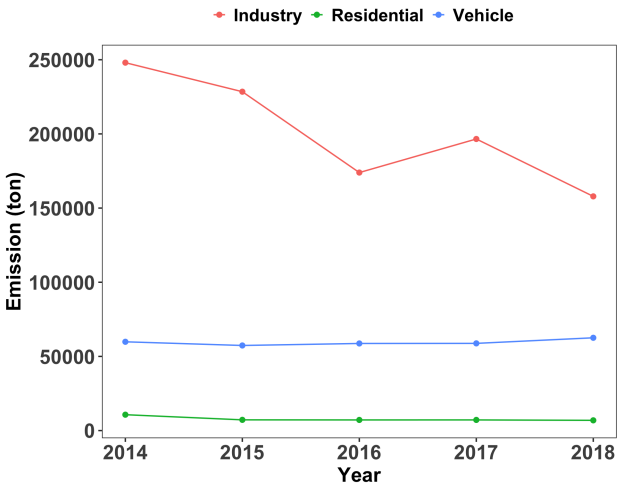

Figure S26: (a) Outputs of main heavy industrial products from 2013 to 2018, (b) SO_2 emissions and (c) nitrogen oxides emissions from 2014 to 2018 in Tangshan.

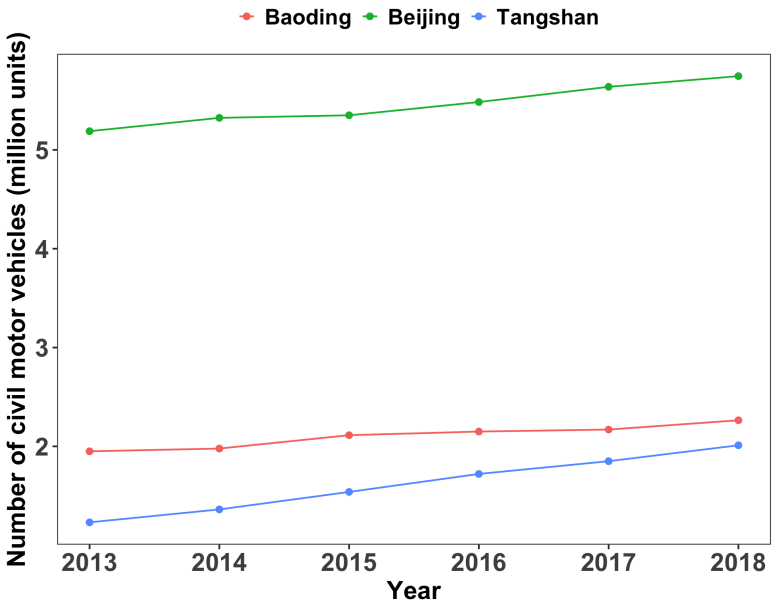

Figure S27: The number of civil motor vehicles from 2013 to 2018 in Baoding (red), Beijing (green) and Tangshan (blue).

Pollutant	Season	Cluster	Adjusted average growth rate(SE, μg/m^3 per hour) and its relative increase (%)					
			2013	2014	2015	2016	2017	2018
$PM_{2.5}$	Spring	Beijing SE	5.3(1), 0	7.7(1.1), 45.8	4(0.4), -24.2	3.1(0.4), -41	2.9(0.3), -45.7	1.8(0.5), -66.4
		Beijing NW	5.8(0.9), 0	4.2(0.9), -26.7	3.1(0.4), -45.5	2.6(0.3), -54.8	3.2(0.7), -45.3	2.1(0.4), -64.2
		Tangshan	6.9(0.8), 0	6.7(0.5), -2.7	6.7(0.7), -1.9	5(0.8), -27.5	4.8(0.4), -29.4	5.2(0.3), -24.6
		Baoding	8.1(1.5), 0	7(0.7), -13.5	5.5(0.7), -32.5	5.5(0.4), -31.8	5(0.4), -38.5	2.5(0.8), -68.9
	Summer	Beijing SE	5.5(0.6), 0	3.1(0.5), -43.9	5.2(0.7), -4.2	2.8(0.2), -48.1	3(0.4), -44.4	1.9(0.2), -64.8
		Beijing NW	4.6(0.4), 0	3.4(0.3), -26.2	3.9(0.5), -15.5	2.8(0.2), -38.5	2.6(0.4), -44	1.7(0.2), -63.4
		Tangshan	3.8(0.8), 0	6.4(0.9), 65.5	4.1(0.7), 6.7	3.1(0.2), -20.2	1.4(0.4), -63.7	3.3(0.6), -14
		Baoding	11.7(1.9), 0	4.5(0.5), -61.7	3.2(0.3), -72.9	3.5(0.4), -70.3	3.4(0.3), -70.6	2.5(0.2), -78.3
	Autumn	Beijing SE	7(0.4), 0	4(0.5), -43.4	6.1(0.6), -12.6	4.6(0.7), -33.9	3.3(0.2), -52.5	3.3(0.4), -52.9
		Beijing NW	5.5(0.5), 0	4.2(0.6), -23.1	5.8(0.7), 5.2	6.9(1.5), 25.5	3(0.4), -46.4	2.4(0.2), -56.9
		Tangshan	11.3(0.9), 0	8.5(0.7), -25	5(0.4), -56.2	6.6(0.6), -41.8	3.7(0.2), -67.4	4.3(0.3), -62.3
		Baoding	11.7(1.2), 0	12.3(1.9), 5.8	6(0.6), -48.3	6(1.1), -48.4	4(0.4), -65.8	3.5(0.5), -69.8
	Winter	Beijing SE	8.1(0.7), 0	11.2(1), 38.2	9.1(0.9), 12.9	9.4(1.4), 15.9	5.4(0.5), -33.5	6.8(0.6), -16.1
		Beijing NW	7.7(0.6), 0	10.2(1.3), 31.6	9.3(1.2), 20.9	9.1(1.2), 18.2	3.6(0.5), -54	5.3(0.4), -31.9
		Tangshan	10.3(0.7), 0	10.3(0.9), -0.2	9.9(0.8), -3.4	8(0.6), -22.4	5.3(0.3), -48.3	4.9(0.4), -52.5
		Baoding	13.8(1.1), 0	13.6(1.7), -1.5	7.7(1.5), -44.6	11.1(1.3), -19.6	5.2(0.5), -62.3	4.1(0.5), -70.2
NO_2	Spring	Beijing SE	5.1(0.8), 0	7.2(0.7), 41.3	6.9(0.7), 36.4	7.2(0.4), 41.5	5.2(0.6), 3.3	3.2(0.2), -37.9
		Beijing NW	6.1(0.6), 0	6.5(0.7), 5.9	7.6(0.7), 24	6.7(0.4), 9.2	7.1(0.8), 16.2	3.8(0.6), -38.8
		Tangshan	6.6(0.7), 0	7.4(0.6), 12.1	8.4(0.8), 27	7(1.1), 6.5	9.2(1.1), 38.8	9.2(0.6), 39
		Baoding	2.3(0.6), 0	6.6(1.2), 190.7	6(0.7), 164.3	6.4(0.5), 182	4.8(0.7), 109.7	2(1.3), -10.8
	Summer	Beijing SE	5.9(0.5), 0	8.5(0.7), 44	4.3(0.5), -27.2	5.7(0.6), -2.8	5.3(0.7), -9.4	4.1(0.4), -30.7
		Beijing NW	7.8(0.5), 0	6.3(0.6), -18.9	5.6(0.4), -28.3	5.9(0.6), -24.2	5.5(0.7), -28.5	3.7(0.3), -51.9
		Tangshan	3.3(0.7), 0	4.1(0.6), 26.5	4.8(0.7), 47	3.9(0.7), 17.8	4.2(1.2), 28.1	3.8(0.5), 16.6
		Baoding	3.4(0.7), 0	1.8(0.3), -46.8	4.3(0.5), 26	2.6(0.4), -24.3	3.8(0.5), 11.7	4.4(0.5), 28.4
	Autumn	Beijing SE	6.9(0.5), 0	6.2(0.4), -10.1	6.5(0.5), -5.1	5.2(0.5), -24.5	5(0.4), -26.8	5.1(0.4), -26.4
		Beijing NW	7.2(0.4), 0	8(0.5), 10.3	7.5(0.6), 4.5	8.4(0.8), 16.6	7.9(0.5), 9.8	6.5(0.4), -10.1
		Tangshan	7.3(0.4), 0	6.1(0.5), -15.3	6.1(0.5), -15.4	7.5(0.7), 3.2	6.9(0.4), -4.5	8(0.3), 10
		Baoding	6.5(0.6), 0	5.5(0.9), -15.3	8.5(0.8), 29.1	7(0.8), 7	4.5(0.4), -32	5(0.3), -22.9
	Winter	Beijing SE	5.9(0.4), 0	7(0.5), 18.3	5.9(0.5), -0.3	6.4(0.5), 7.3	3.5(0.5), -41.7	5.2(0.3), -11.5
		Beijing NW	7.3(0.4), 0	7.6(0.5), 5.1	6.6(0.5), -9.3	7.1(0.4), -1.8	5.2(0.6), -27.8	6.6(0.4), -9.3
		Tangshan	6.3(0.3), 0	7(0.5), 10.4	6.2(0.4), -2.9	7.5(0.5), 17.6	7.3(0.4), 14.7	6.7(0.3), 5.9
		Baoding	6.8(1.1), 0	4.5(0.7), -33.2	5.7(0.4), -15.8	11(0.5), 63	5.8(0.4), -14.9	5(0.3), -26.6
SO_2	Spring	Beijing SE	2(0.4), 0	2.3(0.3), 15.2	1.1(0.1), -43.8	0.6(0.1), -68.7	0.8(0.1), -60.7	0.6(0.3), -70.5
		Beijing NW	2.5(0.3), 0	2(0.5), -19.4	0.8(0.2), -69.4	0.5(0.2), -82	0.6(0.1), -74.6	0.5(0.2), -81.9
		Tangshan	5.9(1.6), 0	4.6(0.8), -22	3.7(0.4), -37.1	7.1(1.9), 20.6	3.1(0.2), -46.7	3.6(0.4), -39
		Baoding	7.3(1.7), 0	11.8(4.2), 61.1	7.9(1.3), 7.7	4.8(0.8), -34.5	6.2(1.4), -14.9	1.4(0.8), -80.9
	Summer	Beijing SE	1(0.2), 0	0.6(0.2), -36.6	0.3(0.1), -71.5	0.1(0), -86.7	0.3(0.1), -75.1	0.4(0), -65.1
		Beijing NW	0.8(0.2), 0	0.8(0.3), 1	0.5(0.2), -37.4	-0.2(0.3), -131.5	0.3(0.1), -58.7	0.2(0.1), -77.5
		Tangshan	2.8(0.8), 0	2.6(0.4), -6.8	3.3(0.7), 19.9	2.4(0.6), -14.9	1.6(0.6), -41.5	1(0.4), -63.3
		Baoding	2.2(0.5), 0	2.4(0.6), 9.5	3.6(0.9), 60.2	2.3(0.2), 2.7	2.7(1.2), 21	1.1(0.2), -52.1
	Autumn	Beijing SE	2.3(0.3), 0	1.2(0.2), -45.6	1(0.1), -56.3	0.8(0.2), -63.1	0.7(0.1), -67.8	0.6(0.1), -71.5
		Beijing NW	2.1(0.4), 0	1.1(0.2), -44.4	1.2(0.2), -43.7	1.3(0.2), -36.1	0.7(0.1), -68	0.3(0.1), -87.1
		Tangshan	4(0.7), 0	1.5(0.6), -63.2	2.1(0.2), -48.2	2.8(0.3), -30.8	2(0.2), -50.5	2.9(0.5), -27.8
		Baoding	4.5(1.5), 0	5.4(1.9), 20	2.2(0.4), -50.6	5.1(0.8), 13.6	3.3(1.1), -27.1	2.9(0.5), -34.7
	Winter	Beijing SE	3.4(0.3), 0	4.3(0.5), 27.6	2.4(0.2), -28.4	2.1(0.4), -36.1	1.1(0.2), -67.4	1(0.1), -71.1
		Beijing NW	3.8(0.4), 0	4.7(0.6), 22.8	2.7(0.2), -28.3	2.4(0.2), -35.8	1.2(0.2), -68.3	0.8(0.1), -80.1
		Tangshan	10.6(0.7), 0	7.4(0.7), -30	5(0.4), -52.7	6.6(0.6), -37.7	3.4(0.3), -67.5	2.6(0.3), -75.1
		Baoding	23.5(3.3), 0	16.9(3.2), -28.1	10.3(1.5), -56.1	10.2(1.2), -56.6	9.6(1.6), -59	3.3(1), -85.9

Table S2: Seasonal and annual adjusted average growth rates (μg/m^3 per hour), their standard errors (SEs) and the corresponding relative increase (%) of adjusted average growth rates based on the level of those in 2013 for $PM_{2.5}$, NO_2 and SO_2 in the first six hours of the calm episodes for each cluster.

Pollutant	Season	Cluster	Adjusted average growth rate in the first six hours				
			Change point	Reduction	Year	Largest reduction	Average (relative) reduction
$PM_{2.5}$	Spring	Beijing SE	2016	2.2(1)	2018	3.5(1.1)	1.4(26.3%)
		Beijing NW	2015	2.6(1)	2018	3.7(1)	2.7(47.3%)
		Tangshan	2016	1.9(1.1)	2017	2(0.9)	1.2(17.2%)
		Baoding	2016	2.6(1.5)	2018	5.6(1.7)	3(37%)
	Summer	Beijing SE	2014	2.4(0.7)	2018	3.5(0.6)	2.2(41.1%)
		Beijing NW	2014	1.2(0.5)	2018	2.9(0.5)	1.7(37.5%)
		Tangshan	2017	2.4(0.9)	2017	2.4(0.9)	0.2(5.1%)
		Baoding	2014	7.2(2)	2018	9.2(1.9)	8.3(70.8%)
	Autumn	Beijing SE	2014	3(0.6)	2018	3.7(0.6)	2.7(39%)
		Beijing NW	2014	1.3(0.7)	2018	3.1(0.6)	1.1(19.1%)
		Tangshan	2014	2.8(1.2)	2017	7.6(1)	5.7(50.5%)
		Baoding	2015	5.6(1.3)	2018	8.1(1.2)	5.3(45.3%)
	Winter	Beijing SE	2017	2.7(0.9)	2017	2.7(0.9)	-0.3(-3.5%)
		Beijing NW	2017	4.2(0.8)	2017	4.2(0.8)	0.2(3%)
		Tangshan	2016	2.3(1)	2018	5.4(0.8)	2.6(25.4%)
		Baoding	2015	6.2(1.9)	2018	9.7(1.2)	5.5(39.6%)
NO_2	Spring	Beijing SE	2018	1.9(0.8)	2018	1.9(0.8)	-0.9(-16.9%)
		Beijing NW	2018	2.4(0.8)	2018	2.4(0.8)	-0.2(-3.3%)
		Tangshan	—	—	—	—	-1.6(-24.7%)
		Baoding	—	—	2018	0.2(1.5)	-2.9(-127.2%)
	Summer	Beijing SE	2015	1.6(0.7)	2018	1.8(0.6)	0.3(5.2%)
		Beijing NW	2014	1.5(0.7)	2018	4(0.6)	2.4(30.4%)
		Tangshan	—	—	—	—	-0.9(-27.2%)
		Baoding	2014	1.6(0.7)	2014	1.6(0.7)	0(1%)
	Autumn	Beijing SE	2016	1.7(0.7)	2017	1.8(0.7)	1.3(18.5%)
		Beijing NW	—	—	2018	0.7(0.5)	-0.4(-6.2%)
		Tangshan	2014	1.1(0.7)	2015	1.1(0.7)	0.3(4.4%)
		Baoding	2017	2.1(0.8)	2017	2.1(0.8)	0.4(6.8%)
	Winter	Beijing SE	2017	2.5(0.7)	2017	2.5(0.7)	0.3(5.6%)
		Beijing NW	2017	2(0.7)	2017	2(0.7)	0.6(8.6%)
		Tangshan	—	—	2015	0.2(0.5)	-0.6(-9.1%)
		Baoding	—	—	2014	2.2(1.3)	0.4(5.5%)
SO_2	Spring	Beijing SE	2015	0.9(0.4)	2018	1.4(0.5)	0.9(45.7%)
		Beijing NW	2015	1.8(0.4)	2016	2.1(0.4)	1.7(65.4%)
		Tangshan	2017	2.7(1.6)	2017	2.7(1.6)	1.5(24.8%)
		Baoding	2018	5.9(1.9)	2018	5.9(1.9)	0.9(12.3%)
	Summer	Beijing SE	2015	0.7(0.2)	2016	0.9(0.2)	0.7(67%)
		Beijing NW	2016	1(0.4)	2016	1(0.4)	0.5(60.8%)
		Tangshan	2018	1.8(0.9)	2018	1.8(0.9)	0.6(21.3%)
		Baoding	2018	1.2(0.6)	2018	1.2(0.6)	-0.2(-8.3%)
	Autumn	Beijing SE	2014	1(0.4)	2018	1.6(0.4)	1.4(60.9%)
		Beijing NW	2014	0.9(0.5)	2018	1.8(0.4)	1.2(55.9%)
		Tangshan	2014	2.5(0.9)	2014	2.5(0.9)	1.8(44.1%)
		Baoding	—	—	2015	2.3(1.6)	0.7(15.8%)
	Winter	Beijing SE	2015	1(0.4)	2018	2.4(0.4)	1.2(35.1%)
		Beijing NW	2015	1.1(0.4)	2018	3(0.4)	1.4(37.9%)
		Tangshan	2014	3.2(1)	2018	8(0.7)	5.6(52.6%)
		Baoding	2015	13.2(3.6)	2018	20.2(3.4)	13.4(57.2%)

Table S3: Years when significant (at 5%) reduction in the adjusted average growth rates as compared to those in 2013 happened and after which the significant increase in the adjusted average growth rate did not happen in subsequent years, together with the amount of the reductions ($\mu g/m^3$ per hour) and their standard errors (SEs) at the years; Years with the largest reduction in growth rates occurred and the amount (SEs), and the average (relative) reduction from 2014-2018. '-' indicates no significant reduction happened.